



**HAL**  
open science

# The Green Microalga *Chlamydomonas reinhardtii* Has a Single $\Delta^3$ Fatty Acid Desaturase That Localizes to the Chloroplast and Impacts Both Plastidic and Extraplastidic Membrane Lipids

Hoa M Nguyen, S. Cuine, Audrey Beyly-Adriano, B. Legeret, Emmanuelle Billon, Fred Beisson, Pascaline Auroy, G. Peltier, Yonghua Li-Beisson

## ► To cite this version:

Hoa M Nguyen, S. Cuine, Audrey Beyly-Adriano, B. Legeret, Emmanuelle Billon, et al.. The Green Microalga *Chlamydomonas reinhardtii* Has a Single  $\Delta^3$  Fatty Acid Desaturase That Localizes to the Chloroplast and Impacts Both Plastidic and Extraplastidic Membrane Lipids. *Plant Physiology*, 2013, 163 (2), pp.914-928. 10.1104/pp.113.223941 . hal-03379102

**HAL Id: hal-03379102**

**<https://hal.science/hal-03379102>**

Submitted on 14 Oct 2021

**HAL** is a multi-disciplinary open access archive for the deposit and dissemination of scientific research documents, whether they are published or not. The documents may come from teaching and research institutions in France or abroad, or from public or private research centers.

L'archive ouverte pluridisciplinaire **HAL**, est destinée au dépôt et à la diffusion de documents scientifiques de niveau recherche, publiés ou non, émanant des établissements d'enseignement et de recherche français ou étrangers, des laboratoires publics ou privés.

# The Green Microalga *Chlamydomonas reinhardtii* Has a Single $\omega$ -3 Fatty Acid Desaturase That Localizes to the Chloroplast and Impacts Both Plastidic and Extrplastidic Membrane Lipids<sup>1[C][W]</sup>

Hoa Mai Nguyen, Stéphan Cui n , Audrey Beyly-Adriano, Bertrand L geret, Emmanuelle Billon, Pascaline Auroy, Fred Beisson, Gilles Peltier, and Yonghua Li-Beisson\*

Commissariat   l'Energie Atomique Cadarache, Institut de Biologie Environnementale et Biotechnologie, Laboratoire de Bio nerg tique et Biotechnologie des Bact ries et Microalgues, Saint-Paul-lez-Durance F-13108, France (H.M.N., S.C., A.B.-A., B.L., E.B., P.A., F.B., G.P., Y.L.-B.); CNRS, UMR Biologie V g tale et Microbiologie Environnementales, Saint-Paul-lez-Durance F-13108, France (H.M.N., S.C., A.B.-A., B.L., E.B., P.A., F.B., G.P., Y.L.-B.); and Aix-Marseille Universit , Saint-Paul-lez-Durance F-13108, France (H.M.N., S.C., A.B.-A., B.L., E.B., P.A., F.B., G.P., Y.L.-B.)

ORCID ID: 0000-0003-1064-1816 (Y.L.-B.).

The  $\omega$ -3 polyunsaturated fatty acids account for more than 50% of total fatty acids in the green microalga *Chlamydomonas reinhardtii*, where they are present in both plastidic and extrplastidic membranes. In an effort to elucidate the lipid desaturation pathways in this model alga, a mutant with more than 65% reduction in total  $\omega$ -3 fatty acids was isolated by screening an insertional mutant library using gas chromatography-based analysis of total fatty acids of cell pellets. Molecular genetics analyses revealed the insertion of a TOC1 transposon 113 bp upstream of the ATG start codon of a putative  $\omega$ -3 desaturase (CrFAD7; locus Cre01.g038600). Nuclear genetic complementation of *crfad7* using genomic DNA containing CrFAD7 restored the wild-type fatty acid profile. Under standard growth conditions, the mutant is indistinguishable from the wild type except for the fatty acid difference, but when exposed to short-term heat stress, its photosynthesis activity is more thermotolerant than the wild type. A comparative lipidomic analysis of the *crfad7* mutant and the wild type revealed reductions in all  $\omega$ -3 fatty acid-containing plastidic and extrplastidic glycerolipid molecular species. CrFAD7 was localized to the plastid by immunofluorescence in situ hybridization. Transformation of the *crfad7* plastidial genome with a codon-optimized CrFAD7 restored the  $\omega$ -3 fatty acid content of both plastidic and extrplastidic lipids. These results show that CrFAD7 is the only  $\omega$ -3 fatty acid desaturase expressed in *C. reinhardtii*, and we discuss possible mechanisms of how a plastid-located desaturase may impact the  $\omega$ -3 fatty acid content of extrplastidic lipids.

Research on lipid metabolism in microalgae has flourished in recent years due to their potential as a rich source of  $\omega$ -3 fatty acids (Guschina and Harwood, 2006; Khozin-Goldberg et al., 2011) and as a feedstock for biodiesel (Hu et al., 2008b; Rosenberg et al., 2008; Beer et al., 2009; Radakovits et al., 2010; Wijffels and Barbosa, 2010; Merchant et al., 2012; Work et al., 2012). Oils

produced by microalgae resemble that of plants (Hu et al., 2008b), with the exception that they contain higher proportions of polyunsaturated fatty acid (PUFA) species (Harwood and Guschina, 2009). Desaturation of acyl groups in glycerolipids is catalyzed by fatty acid desaturases (FADs), which insert a C=C bond at a specifically defined position of an acyl chain (Shanklin and Cahoon, 1998). The degree of unsaturation of fatty acid components largely determines the chemical property and thus the utility of the oils produced. FADs have been one of the major tools for the genetic engineering of oil composition in land crops (Shanklin and Cahoon, 1998; Napier et al., 1999). In view of biodiesel applications, low PUFA content is advantageous in algal oil because of oxidation issues (Frankel, 1991).

With the suites of sophisticated molecular genetic and genomic tools developed in the green microalga *Chlamydomonas reinhardtii* and the existence of substantial literature related to its cell biology, physiology, and biochemistry, this organism has emerged as a major model for research on algal oil (Radakovits et al., 2010; Merchant et al., 2012; Liu and Benning, 2013). Although the understanding of lipid metabolism in *C. reinhardtii*

<sup>1</sup> This work was supported by French Agence Nationale de la Recherche grants (ALGOMICS and DIESALG), by the H lioBiotec platform, funded by the European Union (FEDER), the R gion Provence Alpes C te d'Azur, the French Ministry of Research, and the Commissariat   l'Energie Atomique, and by the Commissariat   l'Energie Atomique for an International Ph.D. studentship (to H.M.N.).

\* Address correspondence to yonghua.li@cea.fr.

The author responsible for distribution of materials integral to the findings presented in this article in accordance with the policy described in the Instructions for Authors ([www.plantphysiol.org](http://www.plantphysiol.org)) is: Yonghua Li-Beisson (yonghua.li@cea.fr).

<sup>[C]</sup> Some figures in this article are displayed in color online but in black and white in the print edition.

<sup>[W]</sup> The online version of this article contains Web-only data.

[www.plantphysiol.org/cgi/doi/10.1104/pp.113.223941](http://www.plantphysiol.org/cgi/doi/10.1104/pp.113.223941)

largely relies on sequence homologies to other models (Riekhof et al., 2005) and is still rather limited compared with the model plant *Arabidopsis* (*Arabidopsis thaliana*; Li-Beisson et al., 2010), functional studies based on mutants have started to provide important insights into the biosynthesis and turnover of membrane and storage lipids in this model alga (Riekhof et al., 2005; Work et al., 2010; Fan et al., 2011; Goodson et al., 2011; Boyle et al., 2012; Li et al., 2012a, 2012b; Yoon et al., 2012).

In *C. reinhardtii*, C16 and C18 PUFAs ( $\omega$ -3 +  $\omega$ -6) make up to 60 mol% of total membrane fatty acids, of which more than 80% are  $\omega$ -3 species (Giroud and Eichenberger, 1988; Siaut et al., 2011). Biochemical evidence for lipid-linked desaturation of fatty acyl chains has been established in *C. reinhardtii* over 20 years (Giroud and Eichenberger, 1989), but only two *C. reinhardtii* mutants affected in fatty acid desaturation have been described to date. These are *crfad6* (*hf-9*), an insertional mutant for the plastidial  $\omega$ -6 desaturase FAD6 (Sato et al., 1995), and microRNA-based silenced lines for the  $\Delta$ 4 desaturase Cr $\Delta$ 4FAD (Zäuner et al., 2012). The putative microsomal  $\Delta$ 12 desaturase FAD2 (Chi et al., 2008) and front-end  $\omega$ -13 desaturase (Kajikawa et al., 2006) have been characterized by heterologous expression in the methylotrophic yeast *Pichia pastoris*, but no mutant is available. Moreover, although  $\omega$ -3 PUFA is the most abundant fatty acid class in *C. reinhardtii*, the  $\omega$ -3 desaturase remains uncharacterized, and no mutant with specific reduction in  $\omega$ -3 content has been isolated so far.

In *Arabidopsis* and *C. reinhardtii*,  $\omega$ -3 PUFAs are present in both plastidic and extraplastidic lipids such as monogalactosyldiacylglycerol (MGDG) and phosphatidylethanolamine (PtdEtn), respectively (Mendiola-Morgenthaler et al., 1985; Giroud et al., 1988). While in plants there are distinct genes for plastidial and extraplastidial  $\omega$ -3 FADs (Wallis and Browse, 2002), only one putative  $\omega$ -3 desaturase seems encoded in the *C. reinhardtii* genome (version 5.0; Merchant et al., 2007). This raises several intriguing possibilities, including the existence of a mechanism to export  $\omega$ -3 acyls from their site of biogenesis to other membranes or a dual localization of the  $\omega$ -3 desaturase homolog (plastid and endoplasmic reticulum [ER]). In this study, we report the identification and characterization of a *C. reinhardtii* mutant defective in the promoter region of the putative

$\omega$ -3 FAD encoded by the Cre01.g038600 locus. We show that while this enzyme is localized to plastids, impairment in its expression leads to a reduction of  $\omega$ -3 fatty acids acylated to both plastidial and ER lipids. Additionally, using plastidial transformation of the mutant, it is demonstrated that the location of this desaturase in the plastid alone is sufficient to ensure normal  $\omega$ -3 fatty acid content in extraplastidic lipids. Possible acyl desaturation and trafficking mechanisms implied by these findings are discussed.

## RESULTS

### Isolation of a Mutant of *C. reinhardtii* with Greater Than 65% Reduction in $\omega$ -3 Fatty Acids

As part of our effort to dissect lipid metabolic pathways in *C. reinhardtii*, an insertional mutant library was generated and screened to isolate mutants with altered fatty acid composition using direct transmethylation of cell pellets and analysis of fatty acid methyl esters (FAMES) by gas chromatography (GC)-flame ionization detection (FID). Among approximately 2,000 mutants screened, we found one (*1C11*) with drastically reduced  $\omega$ -3 fatty acids (Fig. 1). Proportions of all  $\omega$ -3 fatty acids [C16:3(7,10,13), C16:4(4,7,10,13), C18:3(9,12,15), and C18:4(5,9,12,15)] were reduced in *1C11*. A mirrored increase in their  $\omega$ -6 fatty acid precursors C16:2(7,10), C18:2(9,12), C16:3(4,7,10), and C18:3(5,9,12) but no differences for saturated (C16:0/C18:0) and monounsaturated [C16:1(7 or 9) and C18:1(9 or 11)] fatty acids were observed. The mutant *1C11* was renamed for FAD7 (*crfad7*) after the in-depth analyses described below.

In order to determine whether the observed decrease in  $\omega$ -3 fatty acids occurred selectively in some lipid classes, total lipid extracts were separated into individual lipid classes by thin-layer chromatography (TLC) and quantified by densitometry or analyzed for fatty acid composition (Fig. 2). While the total amount of each major glycerolipid class [MGDG, digalactosyldiacylglycerol (DGDG), sulfoquinovosyldiacylglycerol (SQDG), phosphatidylglycerol, PtdEtn, and the betaine lipid 1,2-diacylglycerol-3-O-4'-(*N,N,N*-trimethyl)-homoserine (DGTS)] remained unaffected in the mutant *crfad7* (Fig. 2A), the proportion of each  $\omega$ -3 fatty acid was strongly reduced

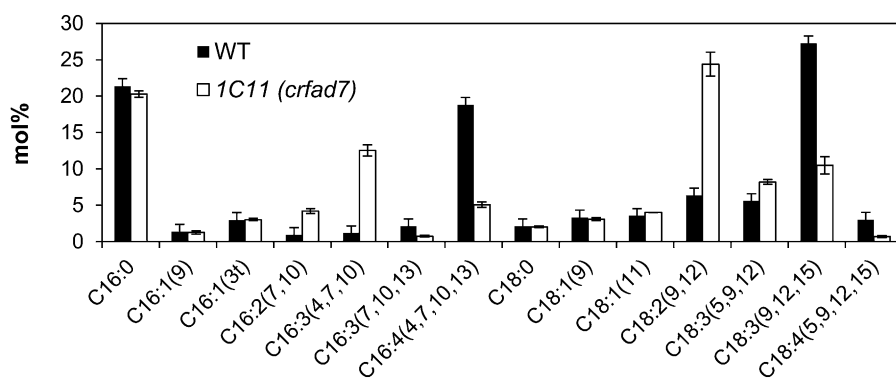


**Figure 1.** Total fatty acid composition of the mutant *1C11* (*crfad7*) and the wild type (WT). Values are shown as mol % of total fatty acids and are means of three biological replicates. Error bars denote 95% confidence intervals. Fatty acids are represented by total carbon numbers:total numbers of unsaturations (position of unsaturations counted from the carboxyl end).

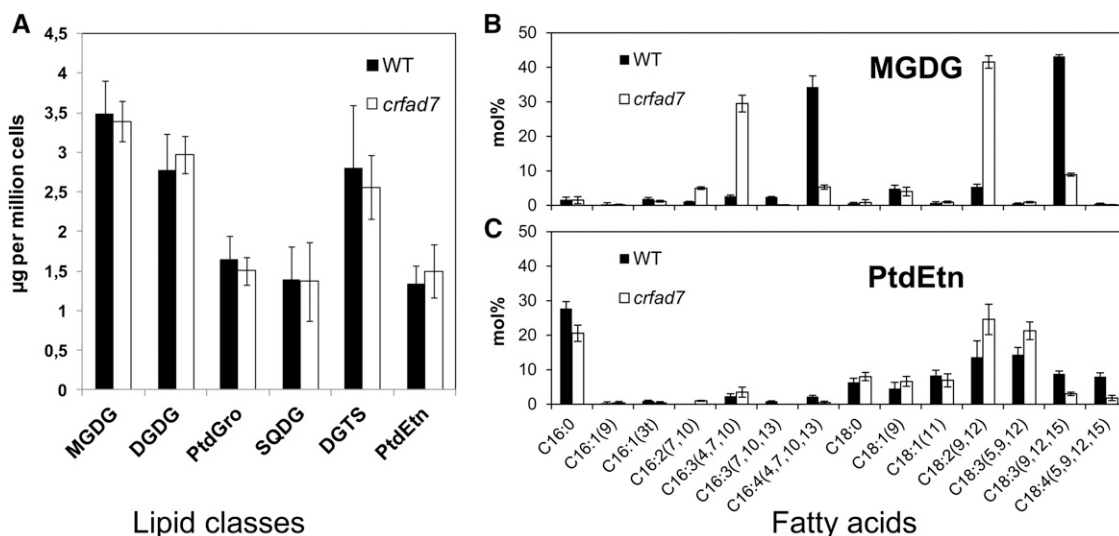


**Figure 2.** Quantification of major membrane lipid classes of the *crfad7* mutant. A, Content of major polar membrane lipids. B, Fatty acid composition of MGDG in the wild type (WT) and the mutant *crfad7*. C, Fatty acid composition of PtdEtn in the wild type and the mutant *crfad7*. Strains were grown under standard conditions. Values represent averages of three biological replicates. Error bars denote 95% confidence intervals.

in all lipid classes, including the nonplastidial lipid PtdEtn (Fig. 2, B and C; Supplemental Fig S1). In storage lipids, such as triacylglycerols (TAGs), the amount of  $\omega$ -3 fatty acids was also reduced but the basal cellular level of TAGs was unaltered in the mutant (approximately  $0.4 \mu\text{g } 10^{-6}$  cells). *crfad7* responded in a similar way to the wild type to nitrogen starvation (i.e. in both backgrounds, TAGs increased more than 10-fold [to approximately  $5 \mu\text{g } 10^{-6}$  cells] after nitrogen starvation for 48 h; Supplemental Fig. S2).

**A Transposon Is Inserted in the Promoter Region of the Locus Cre01.g038600, Encoding a Homolog of the Arabidopsis FAD7  $\omega$ -3 Desaturase**

Since an insertional mutant library was generated by transformation of the *aphVIII* cassette into the wild-type strain 137C, to determine the number of insertions in the mutant genome, Southern-blot analysis was carried out using a labeled *aphVIII* gene encoding resistance to paromomycin as a probe to hybridize the genomic DNA digested by *NotI* (see Supplemental Text S1). As shown in Supplemental Figure S3A, at least two hybridization signals were detected, suggesting multiple insertions of the *aphVIII* gene. In order to establish a genetic link between the observed fatty acid phenotype and the insertion of an antibiotic resistance cassette, the *crfad7* mutant (*mt<sup>-</sup>*) was back-crossed with the wild-type strain CC125 (*mt<sup>+</sup>*) and the progenies were analyzed. Fourteen complete tetrads were obtained and analyzed for fatty acid composition and paromomycin resistance. Progeny of several tetrads showed modified fatty acid composition but were sensitive to paromomycin. An example of such a tetrad is shown in Supplemental Figure S3B. These data demonstrated that the altered fatty acid phenotype

did not result from an *aphVIII* insertion, which made it impossible to identify the mutated gene via classical techniques based on the amplification and sequencing of flanking regions of the cassette. Nonetheless, based on the strong reduction in  $\omega$ -3 fatty acids and on the concomitant increase in  $\omega$ -6 fatty acids, it seemed very likely that the affected locus in the mutant genome encoded an  $\omega$ -3 FAD (this enzyme catalyzes the formation of a double bond in the  $\omega$ -3 position of an existing  $\omega$ -6 fatty acid). BLAST searches of the *C. reinhardtii* genome version 5.0 (Merchant et al., 2007) using the three Arabidopsis  $\omega$ -3 FADs and the single cyanobacterial DesB  $\omega$ -3 FAD as baits identified only one homolog in *C. reinhardtii* (locus Cre01.g038600). A full-length transcript supporting the gene model prediction could be assembled from EST by mapping several transcriptomic data sets available through the University of California Los Angeles Genome Browser hosted at <http://genomes.mcdb.ucla.edu/Cre454/index.html>, which supports the gene model prediction and confirms that the encoded protein is indeed expressed.

The predicted protein coded by Cre01.g038600 showed sequence similarity first to AtFAD7 (63.1% identity) followed by AtFAD8 (60.8% identity) and AtFAD3 (56.6% identity). It consists of 418 amino acids, with three regions of highly conserved His box motifs, which are typical of all membrane-bound desaturases (Fig. 3). Eight His residues present in these His boxes were reported previously as HX<sub>3,4</sub>H, HX<sub>2,3</sub>HH, and HX<sub>2,3</sub>HH (Shanklin and Cahoon, 1998; Nakamura and Nara, 2004). These His residues are supposed to coordinate with two iron atoms and act at the catalytic center of desaturases. The encoded protein is also predicted by the software TMHMM (Krogh et al., 2001) as a membrane protein containing three transmembrane regions.

This is similar to the situation for other  $\omega$ -3 FADs (Los and Murata, 1998). Another feature of the CrFAD7 protein is the presence of an 18-amino acid N-terminal transit peptide for plastid targeting, as predicted by PredAlgo, a protein subcellular localization tool dedicated to green algae (Tardif et al., 2012). These observations indicated that the protein coded by the locus Cre01.g036800 possessed all the typical features of a membrane-bound desaturase and was likely located in the plastid.

To test if any potential modifications (insertions/deletions/rearrangement, etc.) occurred in the mutant genomic DNA around the locus Cre01.g038600, a PCR-based approach was used to amplify the region. The PCR product was approximately 5 kb larger when the mutant genomic DNA was used as a template, as compared with that of wild-type DNA (Fig. 4A). Sequencing of the PCR product amplified from the mutant background revealed the presence of a transposable element (i.e. transposon) located 113 bp upstream of the ATG start codon of Cre01.g038600 (Fig. 4B). Sequence BLAST searches identified this transposon as a previously characterized 5.7-kb TOC1 transposon of *C. reinhardtii* (Day and Rochaix, 1991), which is consistent with the increase in the size of the PCR product amplified from the mutant. The copy number of TOC1 in the genome of *C. reinhardtii* varies from strain to strain, with the wild-type strain 137C harboring around 35 to 40 copies of TOC1 per genome (Day et al., 1988). Due to its relatively high copy number, the frequency of random exchange between regions of DNA caused by environmental factors also increased. Although other possibilities exist, the simplest explanation is that during the process of mutagenesis (i.e. electroporation), a copy of the TOC1 transposable element may have jumped to the promoter region of the locus Cre01.g038600, thus creating the mutant *crfad7*.

Determination of mRNA levels by quantitative reverse transcription (RT)-PCR showed that the transcript Cre01.g038600 was strongly reduced (more than 90%) in *crfad7* compared with the wild type (Fig. 4C),

**>CrFAD7**

cTP

MQCLSRSSLRAPT LSTRARAAPVLRSSVVKVANVAIPEAPQQDRFKRNADGTYDLSAPP

FTLQDLRNAIPAHCWENKFRSM AHLALDVGIVFLAAVAFTVNQWWWPLYVVAQG

TMFWALFVVGHHDCGHQSFNSNKALNDFIGHLTHSSILVPYHGWRISHRTHHANHGHHVEN

Box 1 Box 2

DESWHVPVTKKLYDHLPEMARVGRLSMPWALFAFPFYLWKRSPGKESHYDPECDLFTAEE

RNQLVTTNAYMLGMVAVLAACIAKLGPLAMFNLYLIPYWINVWVLDIVTYLHHGSHDQDN

EKMPWYRGEESYLRGGLTTIDRDYGFNFKIIHHDIGTHVVHHLFPQIPHYNLEEAETAVKP

Box 3

VMGPYYREPMKSPGLPHTLVEPLRSFTNDHYVADSGDIVYQKDPNFPVSGKAVAGKA

**Figure 3.** Structural features of CrFAD7. The presence of three conserved His boxes, a typical feature of membrane-bound desaturases, is underlined. The predicted chloroplast transit peptide (cTP) is boxed in the N terminus.

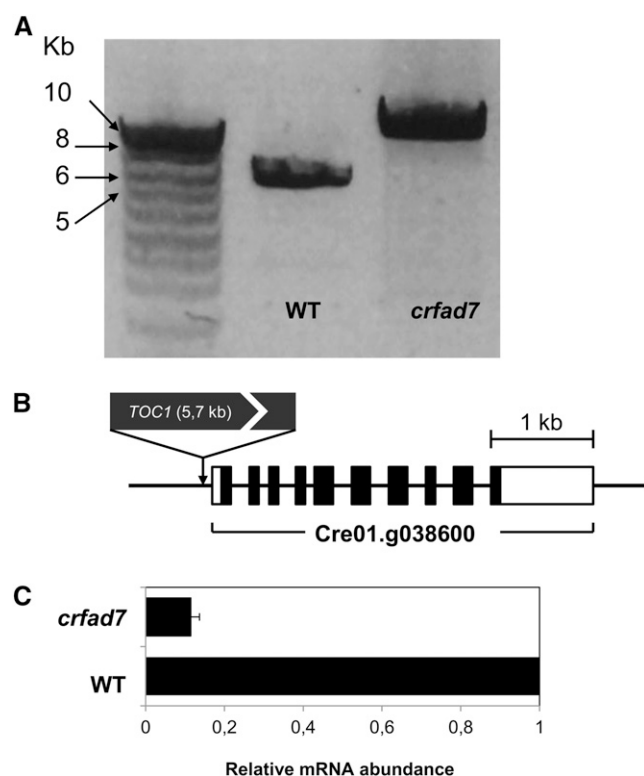


**Figure 4.** Molecular genetic analyses of the mutant *crfad7*. A, PCR amplification of the Cre01.g038600 sequence from genomic DNA prepared either from the wild type (WT) or the *crfad7* mutant. B, Insertion of the transposon TOC1 113 bp upstream of the ATG start codon of Cre01.g038600 in the mutant *crfad7* revealed after DNA sequencing of the PCR product. C, Quantitative RT-PCR analyses of the transcript level of *CrFAD7* in the wild type and the mutant *crfad7*. Expression levels of *CrFAD7* were normalized to the housekeeping gene *RACK1* and compared with the level in the wild type (set to 1). Error bars represent SD based on three biological replicates, each biological replicate consisting of three technical replicates.

consistent with the observed reduction in  $\omega$ -3 fatty acid content in the mutant.

#### The *crfad7* Mutant Is Complemented by Nuclear Transformation with Genomic DNA Containing Cre01.g038600

To demonstrate that the observed mutant phenotype is due to alterations in the locus Cre01.g038600, transformation of the nuclear genome of the *crfad7* mutant was performed using the genomic DNA of 3,944 bp starting from the ATG codon of the locus Cre01.g038600 and including also the 3' untranslated region. The gene was cloned into pSL-Hyg vector, containing the *aphVII* gene conferring resistance to hygromycin. After screening about 400 drug-resistant clones by GC-FID, several clones showing wild-type-like fatty acid compositions (i.e. complementation) were isolated (Fig. 5). Quantitative RT-PCR analyses confirmed the restored transcripts for the corresponding gene in the complemented lines (Supplemental Fig. S4). This result demonstrated that

the strong reduction in  $\omega$ -3 fatty acids observed in the *crfad7* mutant was indeed due to the impairment in CrFAD7 expression.

**CrFAD7 Is Localized to Plastid by Immunofluorescence in Situ Hybridization**

The fact that the mutation in CrFAD7 impacted some lipid molecular species present only in plastids or some others specific to the ER suggested that  $\omega$ -3 desaturated acyl chains were either transported across subcellular compartments or the enzyme had multiple subcellular locations. To address this question, we localized this protein using an immunohybridization technique. The CrFAD7 gene was cloned and expressed as a C-terminal fusion to the triple influenza hemagglutinin epitope (3xHA; Fig. 6A). The hemagglutinin (HA) epitope has been widely used for the subcellular localization of proteins in *C. reinhardtii* (Silflow et al., 2001; Lechtreck et al., 2009). To rule out any possibility of protein mistargeting, the tagged protein was expressed in the nuclear genome of the mutant *crfad7*, and only hygromycin-resistant clones showing a wild-type level of  $\omega$ -3 fatty acid content were subjected to immunoblot analysis.

Western blots of fractionated total cellular proteins against anti-HA antibodies revealed the presence of CrFAD7 in the membrane protein fraction but not in the soluble protein fraction (Fig. 6B), which showed that CrFAD7 is a membrane protein like all the other characterized  $\omega$ -3 desaturases (Shanklin and Cahoon, 1998). We then proceeded to immunolocalization using in situ hybridization and microscopic examination with a laser scanning confocal microscope (Fig. 6C). High-fluorescence signals of the anti-HA antibodies were always found to be overlapping with chlorophyll autofluorescence; thus, dual targeting to mitochondria is not likely. These observations suggested that CrFAD7 was localized only to the plastid.

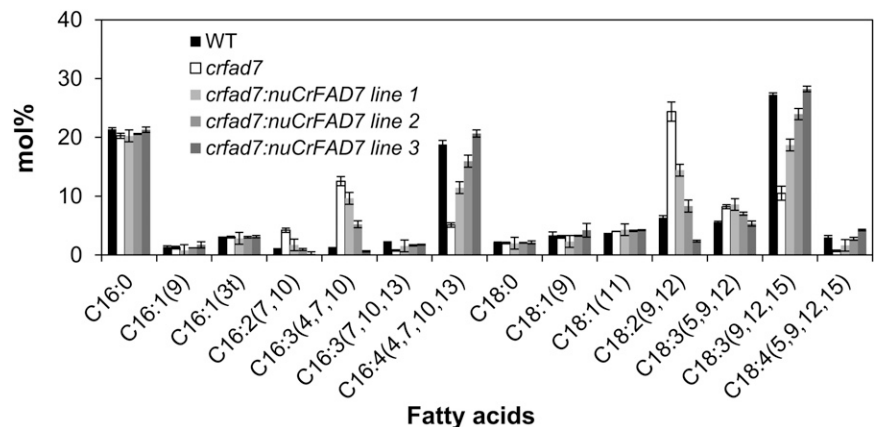
**Plastidial Expression of CrFAD7 Restores  $\omega$ -3 Fatty Acids in All Lipid Molecular Species**

To determine whether plastidial localization alone would be sufficient to fully restore  $\omega$ -3 fatty acid content

in extraplastidic molecular species in addition to plastidic ones, and also to further confirm that a dual localization was not necessary, we attempted to complement the *crfad7* mutant via introduction of the gene CrFAD7 into the chloroplast genome and performed lipidomic analysis. Considering preferential codon usage, to ensure optimal expression of CrFAD7 in the plastid genome, the complementary DNA encoding CrFAD7 was codon optimized and resynthesized. The resulting construct was integrated into the plastid genome of the *crfad7* mutant under control of the plastidial *psaA* promoter via biolistic bombardment. Fatty acid composition analyses of spectinomycin-resistant clones identified several independent lines that showed similar total fatty acid composition to that of the wild type (Supplemental Fig. S5).

To check that the plastidial expression of CrFAD7 alone allows full recovery of the mutant to a wild-type fatty acid composition in all lipid molecular species, a comparative lipidomic analysis using ultra-performance liquid chromatography (UPLC) coupled with tandem mass spectrometry (MS/MS) was performed. Under negative ionization mode, more than 80 polar lipid species were identified in wild-type cells cultivated under standard conditions (Fig. 7). The shift from highly polyunsaturated species to less unsaturated species is observed in the mutant *crfad7*. For example, MGDG (18:3-16:4) reduced in the mutant with an concomitant increase in MGDG(18:2-16:3), and DGTS(18:4-16:0) decreased whereas DGTS(18:3-16:0) increased in *crfad7*. The overall pattern of reduction in  $\omega$ -3 and increment in  $\omega$ -6 fatty acids is straightforwardly reflected in the individual plastidic lipid species (MGDG, DGDG, phosphatidylglycerol, and SQDG). It is somehow more complex in the interpretation of the ER lipids (DGTS and PtdEtn); this is partly due to the preferential presence of  $\omega$ -6 C18:3(5,9,12) fatty acid, which is largely absent in plastidial membranes (Giroud et al., 1988), and partly because with the current technique we could not yet differentiate the  $\omega$ -6 trienoic acid C18:3(5,9,12)-containing species from the  $\omega$ -3 trienoic acid C18:3(9,12,15)-containing species. Nonetheless, all the C18:4(5,9,12,15)-containing PtdEtn and DGTS species are always reduced

**Figure 5.** Complementation of *crfad7* by nuclear expression of CrFAD7. Fatty acid composition analyses for three independent nuclear complementation lines are shown. Values are means of three biological replicates, and error bars represent 95% confidence intervals. WT, Wild type.



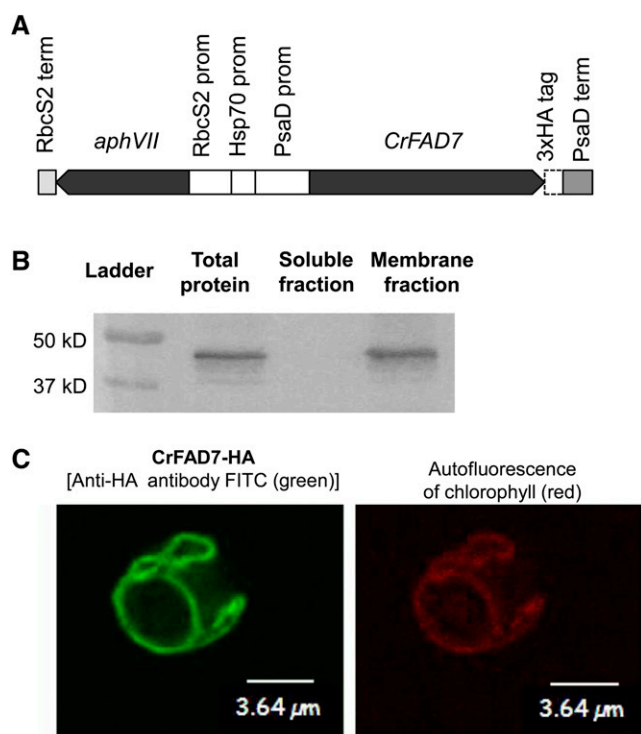


**Figure 6.** Subcellular localization of CrFAD7 by immunofluorescence analysis. A, CrFAD7 protein is fused to 3xHA in its C terminus. B, Western-blot analysis of total cellular protein, soluble fraction, and membrane fraction using the anti-HA antibodies. Proteins extracted from one representative complemented line are shown. C, Confocal images of the *crfad7* mutant when complemented by CrFAD7-HA. Cells were excited at 488 nm, and emission was collected at 498 to 515 nm for FITC and at 656 to 714 nm for chlorophyll. [See online article for color version of this figure.]

in the mutant *crfad7*. Most importantly, in the plastidial (and nuclear) complemented lines, restoration of 18:4 and 16:4 fatty acids to wild-type levels was observed for the species containing such fatty acids, including the extra-plastidic species PtdEtn(18:4-18:0). It is also easily seen from this analysis that the proportion of each lipid molecular species was restored to wild-type levels in both nucleus- and plastid-complemented lines. Taken together, this analysis clearly shows that the expression of CrFAD7 in the plastid alone results in normal fatty acid content in the ER and argues against a dual localization of this protein.

#### CrFAD7 Transcription Is Regulated by Light and Temperature

To probe potential physiological functions of CrFAD7, we examined how environmental factors regulate its transcription. Quantitative RT-PCR analyses of transcription levels of the light- versus dark-grown cells revealed that CrFAD7 transcription was activated by light and repressed in dark-grown cells (Fig. 8A). This was consistent with the increased proportion of trienoic acids in light-grown cells (Fig. 8B). Light-induced

expression of FAD genes has previously been reported for the cyanobacterium *Synechocystis* sp. PCC6803 as well as for higher plants (Kis et al., 1998). We also observed that the transcript level of CrFAD7 is suppressed over 50% when cultivated at 35°C as compared with the usual growth temperature (25°C; Fig. 8C). When cells were cultivated at a lower temperature (15°C), its transcription increased slightly, but below the threshold of statistical significance (i.e. less than 2-fold). A significant reduction of  $\omega$ -3 fatty acids concomitant with an increase in  $\omega$ -6 fatty acids and monounsaturated fatty acids was observed at 35°C, whereas no difference was found when cells were cultivated at 15°C (Fig. 8D).

Furthermore, the fatty acid composition of the mutant was observed when cells were cultivated at 25°C or at 15°C (Supplemental Fig. S6). This result was contrary to what has been observed in the *Arabidopsis atfad7* mutant, where changes in fatty acid composition were minor when *atfad7* was grown at a lower temperature (i.e. 18°C; Browne et al., 1986a) compared with its normal growth temperature (22°C). This was explained later by the discovery of the temperature-sensitive locus *fad8* in *Arabidopsis* that restored the level of  $\omega$ -3 fatty acids at lower temperatures (McConn et al., 1994). The fact that the *crfad7* mutant phenotype was observed also in lower temperatures ruled out the existence of an equivalent form of FAD8 in *C. reinhardtii*, thus supporting the occurrence of a single  $\omega$ -3 desaturase.

#### *crfad7* Shows Enhanced Short-Term Thermotolerance Compared with the Wild Type

Under standard growth conditions (light intensities of 100  $\mu\text{mol photons m}^{-2} \text{s}^{-1}$ , 25°C), *crfad7* is indistinguishable from the wild type in terms of cell size, growth rate, and chlorophyll content (Supplemental Fig. S7). We did not observe any difference in growth between the wild type and the mutant when cultivated at 15°C. Since the transcription of CrFAD7 in the wild type is suppressed at higher temperatures (Fig. 8), we measured photosynthetic activities of mutant and wild-type cells following an incubation of 30, 40, or 60 min at this temperature. As can be seen in Figure 9, PSII activities, measured as the proportion of absorbed energy used in photosynthesis compared with total absorbed energy ( $F_v/F_m$ ), decreased at a slower rate in *crfad7* than in the wild type. After 60 min of cultivation at 45°C, PSII in the wild-type strain was completely impaired, whereas approximately 20% of initial PSII activities still remained in the mutant. During this period, the fatty acid composition of both wild-type and mutant cells remained unchanged (Supplemental Fig. S8).

#### DISCUSSION

In this study, we report the isolation and characterization of a mutant impaired in  $\omega$ -3 fatty acid synthesis. We provide biochemical and molecular genetic evidence that the affected locus, Cre01.g038600, encodes a

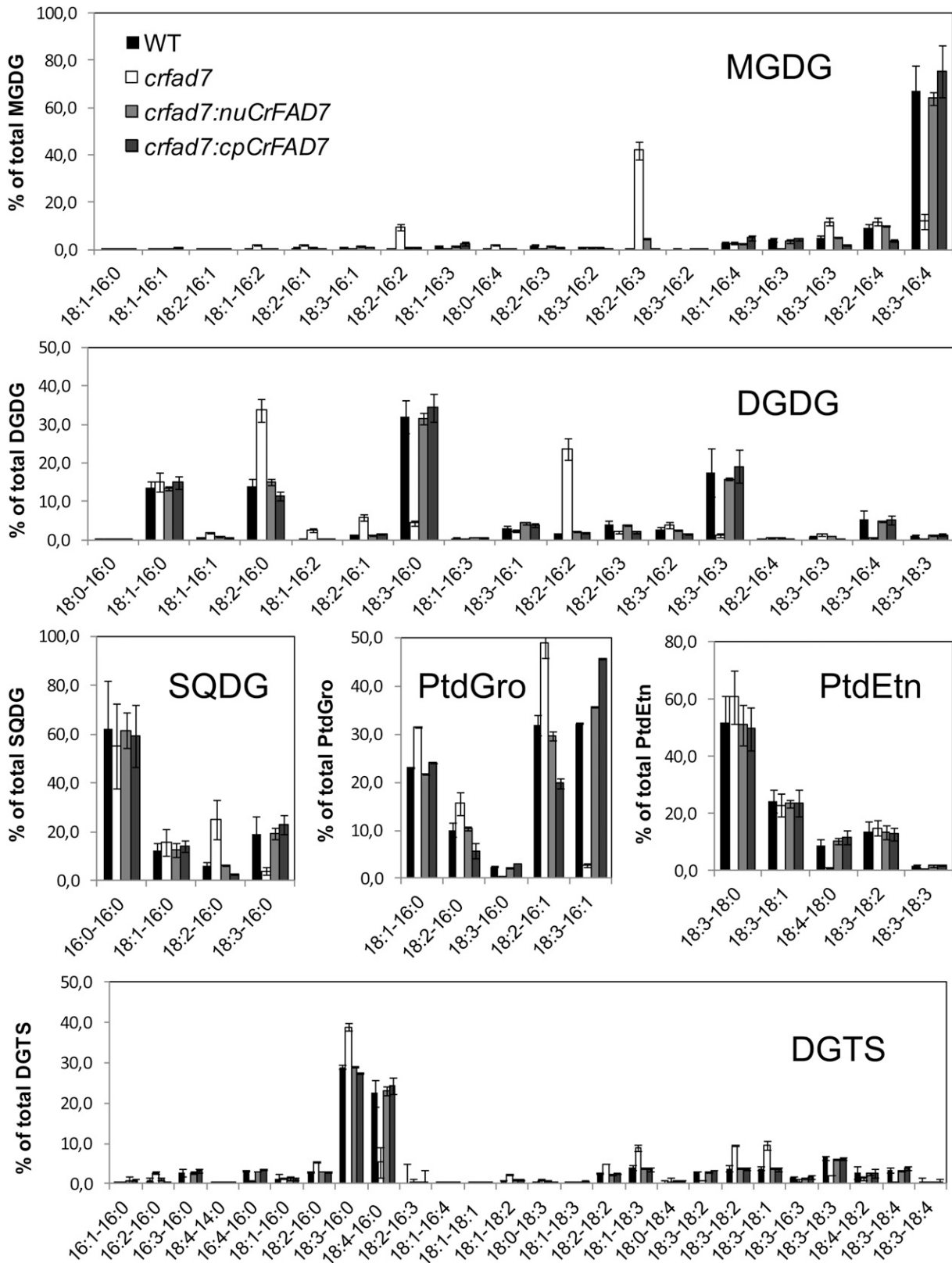


**Figure 7.** Analysis of lipid molecular species of the wild type, *crfad7*, and the nuclear and plastidial complemented lines. Relative abundance for each lipid molecular species is shown. (The complete data set is also presented in Supplemental Table S1.) It is calculated as an area percentage of all molecular species present in that particular lipid class. Values are means of three biological replicates and two technical replicates, and error bars represent 95% confidence intervals. *crfad7:cpCrFAD7*, plastidial complemented lines; *crfad7:nuCrFAD7*, nuclear complemented lines. Note that the stereospecific position of each acyl group on the glycerol backbone could not be assigned.

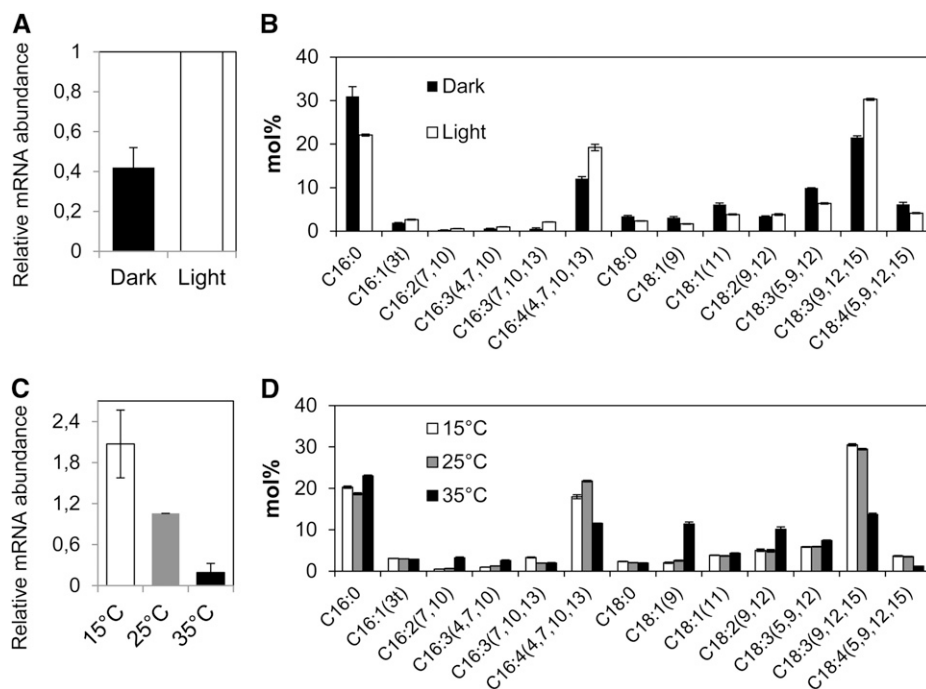


**Figure 8.** Regulation of  $\omega$ -3 fatty acid synthesis by light and temperature in wild-type *C. reinhardtii*. A, Quantitative RT-PCR analyses of *CrFAD7* transcript for wild-type cells when cultivated in the light or under dark. B, Fatty acid compositional analysis of the cells harvested from light- or dark-grown cultures. C, Quantitative RT-PCR analyses of *CrFAD7* transcript for wild-type cells when cultivated at 15°C, 25°C, and 35°C. D, Fatty acid compositional analysis of the cells after being subjected to 15°C, 25°C, and 35°C for 48 h. Wild-type cells were cultivated in TAP medium at 25°C until midlog phase, then they were either subjected to changes in luminosity (in the dark or under a light intensity of 100  $\mu\text{mol photons m}^{-2} \text{s}^{-1}$ ) or transferred to two other temperatures (15°C or 35°C) for 48 h before being sampled for analyses. Error bars represent sd based on three biological replicates. Transcription level was calculated the same way as described in Figure 4C.

functional  $\omega$ -3 FAD, named CrFAD7. We show that CrFAD7 localizes to the chloroplast and demonstrate that this subcellular location alone is sufficient to provide extraplastidial membranes with a normal content of  $\omega$ -3 fatty acids. Below, we discuss the occurrence and expansion of members belonging to the  $\omega$ -3 FAD families during evolution of the green lineage and present possible mechanisms of  $\omega$ -3 fatty acid distribution into the various types of *C. reinhardtii* membranes.

#### *C. reinhardtii* Has a Single $\omega$ -3 FAD Localized to Plastids

BLAST searches of the genome of *C. reinhardtii* (Merchant et al., 2007) identified only one gene encoding a putative plastidial  $\omega$ -3 FAD (Cre01.g038600). No other desaturase that may correspond to a homolog of the Arabidopsis cytosolic isoform AtFAD3 (Riekhof et al., 2005) or to a homolog of the second Arabidopsis plastidial isoform, AtFAD8, could be found in the current curated genome (version 5.0). The fact that the expression of *CrFAD7* in the plastid only was sufficient to restore the normal supply of  $\omega$ -3 fatty acids to extraplastidial membranes strongly supported the view that this protein was the only  $\omega$ -3 desaturase in *C. reinhardtii*. Interestingly, the presence of a single plastid-located  $\omega$ -3 desaturase may not be unique to *C. reinhardtii* among microalgae. BLASTP searches in the Chlorophyceae

microalgae with fully sequenced genomes (*Chlorella variabilis* NC64A, *Coccomyxa subellipsoidea* C-169, and *Volvox carteri*) revealed the presence of only one homolog of CrFAD7 in each species (Table I). Furthermore, prediction of the potential subcellular locations for these proteins using the algorithm PredAlgo showed that in all three other species, as in *C. reinhardtii*, the  $\omega$ -3 desaturase is targeted to plastid, but they differ in the length of transit peptide (Table I).

Immunolocalization studies based on examination of a fusion of CrFAD7 to 3xHA showed that CrFAD7 is located to the plastids, including both thylakoid and envelope membranes. This is further supported by the identification of several peptides belonging to the CrFAD7 protein in a proteomic study on isolated *C. reinhardtii* plastids (Terashima et al., 2011). The idea that CrFAD7 is present in the thylakoid membranes in addition to the plastidial envelopes is further supported by a previous study of the soybean (*Glycine max*) FAD7 (GmFAD7), which showed that this protein is present in both membranes of the plastids (Andreu et al., 2007), and also by the localization of the cyanobacterial DesB, the ancestral form of  $\omega$ -3 FADs, to both thylakoids and the cytoplasmic membrane (i.e. the membrane at the origin of the inner plastid envelope in organisms of the green lineage; Mustardy et al., 1996).

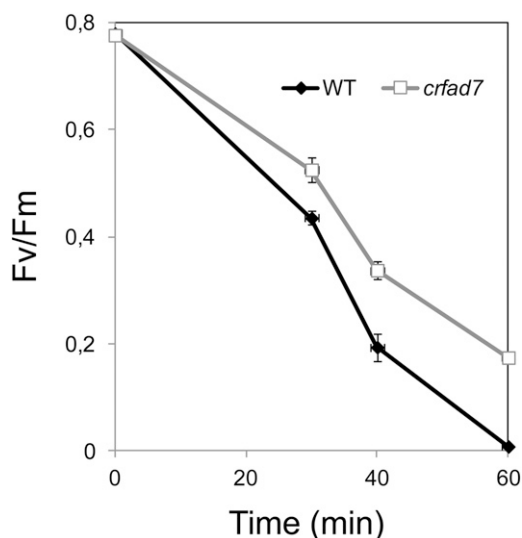


**Figure 9.** Low  $\omega$ -3 fatty acid content causes PSII to be more tolerant to high temperature. The effect of short exposure to high temperature (45°C) on the photosynthetic efficiencies of the wild type (WT) and the *crfad7* mutant as measured by the chlorophyll fluorescence parameter  $F_v/F_m$  after 0, 30, and 60 min of growth at 45°C is shown. Error bars represent SD based on three biological replicates.

### Fatty Acid Desaturation and Expansion of the $\omega$ -3 FAD Family

Previous phylogenetic analyses of cyanobacteria and plant membrane-bound desaturases have suggested a common ancestral origin of the plastidial and ER-located  $\omega$ -3 desaturase isoforms in plant cells (Sperling et al., 2003). To look into the evolutionary relationship of  $\omega$ -3 FAD family proteins, a phylogenetic tree was constructed based on the alignment of amino acid sequence of desaturases from several plants, microalgae, and also cyanobacteria species. A neighbor-joining tree using the  $\omega$ -6 FAD from the cyanobacterium *Synechocystis* sp. PCC 6803 as a root is presented in Supplemental Table S2. This analysis showed that CrFAD7 clusters together with other microalgal FADs of the Chlorophyceae class (*C. variabilis* NC64A, *C. subellipsoidea* C-169, and *V. carteri*) but subbranched from the non-Chlorophyceae species, including *Micromonas* sp. and *Phaeodactylum tricorutum*. The neighbor-joining tree also shows that CrFAD7 is more closely related to the ancestral cyanobacterial homolog DesB than the second plastidial isoform FAD8 and the ER-specific isoform (FAD3), indicating that the latter two isoforms present in higher plants occurred later in evolution. Multiple isoforms of  $\omega$ -3 FAD appear to be a characteristic of higher plants and mosses, while in green algae and cyanobacteria, a single form of this enzyme is found. For example, in the model plant *Arabidopsis*, three  $\omega$ -3 desaturases localized in two subcellular compartments are present: AtFAD3 is ER specific (Arondel et al., 1992; Dyer and Mullen, 2001), while AtFAD7 and AtFAD8 are plastid located (Browse et al., 1986b; McConn et al., 1994). These isoforms seem to

exhibit preferential expression patterns in some organs; for example, AtFAD7/AtFAD8 is highly expressed in green tissues, whereas AtFAD3 is largely present in seeds (Winter et al., 2007). This suggests that expansion of the  $\omega$ -3 FAD family from only one member to three or even more must have occurred after the first endosymbiosis and is likely linked to the development of multicellularity.

### Possible Mechanisms for $\omega$ -3 Fatty Acid Distribution into Plastidic and Extrplastidic Membrane Lipids

Evidence presented in this study suggested that one locus, Cre01.g038600, is responsible for the desaturation of  $\omega$ -6 fatty acids present in all lipid molecular species (Fig. 7), regardless of their subcellular localization. We further demonstrated that CrFAD7 is the single  $\omega$ -3 FAD and that it is located in the plastids (envelopes plus thylakoid membranes). Lipid-linked acyl desaturation is a well-known mechanism and has been characterized in higher plants, as has also been demonstrated in *C. reinhardtii* through substrate-labeling studies (Giroud and Eichenberger, 1989). Each membrane system often has its own characteristic acyl-lipid composition; for example, the galactolipids (MGDG and DGDG) and the sulfolipid SQDG are only associated with plastidial membranes, whereas PtdEtn is present in endomembrane systems. This compartment-specific location for a particular lipid class requires the desaturation of its acyl chains in a location-specific manner, or an efficient acyl-shuffling mechanism must operate. For example, in *Arabidopsis*, it is well known that the ER-located AtFAD3 desaturase (Dyer and Mullen, 2001) converts 18:2-Phosphatidylcholine (PtdCho) to 18:3-PtdCho, whereas the plastid-located AtFAD7/AtFAD8 (Andreu et al., 2007) desaturates 18:2-MGDG to 18:3-MGDG. This raises the question of how the single enzyme CrFAD7 can desaturate acyl chains attached to lipid species present across several subcellular compartments.

Based on our current knowledge of lipid synthesis and transport, this finding could be explained in several ways. One of the working hypotheses is that the presence of this single desaturase in the plastid envelopes of *C. reinhardtii* would potentially allow CrFAD7 to have access to both plastidial and ER-located lipid substrates through the ER-plastid contact site (Fig. 10A, red box). The concept of glycerolipid transfer via interorganelle contact site is not new; indeed, the ER-plastid contact site has been observed with a microscope using optical tweezers (Andersson et al., 2007). This subject has been intensively reviewed by Jouhet et al. (2007). The central role of the ER-plastid junction in cellular lipid metabolism has previously been shown in other studies on TAG biosynthesis in *C. reinhardtii* (Fan et al., 2011; Goodson et al., 2011). This location will also allow the desaturation step to be integrated to other reactions present in plastid envelopes, which are major sites of the assembly of “prokaryotic-type” membrane lipids, and also the sites where extensive acyl-editing or acyl-remodeling enzymes locate (Joyard et al., 1998; Rolland

**Table 1.** Number, identity, and predicted subcellular localization of putative  $\omega$ -3 FADs in the Chlorophyceae microalgal species with sequenced genomes

Protein subcellular localization is predicted by the PredAlgo program (<https://giavap-genomes.ibpc.fr/cgi-bin/predalgotdb.perl?page=main>). PredAlgo computes a score for three subcellular compartments: the mitochondrion (M), the chloroplast (C), and the secretory pathway (SP). The assigned target compartment is the one with the highest score. JGI, Genome portal hosted at the Joint Genome Institute.

Microalgae Species	No. of Putative $\omega$ -3 Desaturases	Abbreviation	PredAlgo Score			Subcellular Compartment	Transit Peptide	Identifier (Locus Name Used in Phytozome or JGI)
			M	C	SP			
<i>C. reinhardtii</i> version 5.0	1	CrFAD7	0.16	3.65	0.08	Chloroplast	18 Amino acids	Cre01.g038600
<i>C. variabilis</i> NC64A version 1.0	1	CnFAD7	1.16	3.50	0.03	Chloroplast	39 Amino acids	estExt_Genewise1.C_430002
<i>C. subellipsoidea</i> C-169 version 2.0	1	CosFAD7	0.48	2.90	0.44	Chloroplast	36 Amino acids	estExt_Genemark1.C_130077
<i>V. carteri</i> version 2.0	1	VcFAD7	0.01	3.62	0.01	Chloroplast	34 Amino acids	Vocar20009411m.g

et al., 2012). Alternatively, but not exclusively, it could also be that  $\omega$ -6 fatty acids are desaturated entirely in the plastid when they are linked to plastidic glycerolipids; subsequently, they are transferred to extraplastidic lipids via the route used by the classical 16:0/18:0/18:1 acyl chains or via the hydrolysis of lipids followed by the formation of 18:3 in the plastid envelope (Fig. 10B). For example, this could be catalyzed by a newly identified lipase (i.e. PGD1), which is specific for galactoglycerolipids in *C. reinhardtii* (Li et al., 2012a).

Although specific ER-located  $\omega$ -3 desaturase isoforms have evolved in plants, the fact that the *atfad2* mutant of *Arabidopsis* contains relatively high levels of 18:3 ( $\omega$ -3) fatty acid in the ER lipids (Miquel and Browse, 1992) suggests that the mechanism in *C. reinhardtii* allowing the transfer of  $\omega$ -3 acyl chains from plastidic to extraplastidic membranes has been conserved in plants.

### Short-Term Thermotolerance in Mutants with Low Levels of $\omega$ -3 Fatty Acids

It is well recognized that photosynthetic plastids are derived from the first endosymbiosis, where an ancestral cyanobacterium was engulfed by a heterotrophic

protist (Reyes-Prieto et al., 2007). This evolutionary deduction is largely supported by the conservation of metabolic pathways from cyanobacteria to eukaryotic green algae to higher plants. One notable example is the conservation of acyl-lipid desaturation reactions and the importance of trienoic acids in membrane functions (Wallis and Browse, 2002). In this study, we found that high  $\omega$ -3 fatty acid content is not beneficial to cells cultivated at higher growth temperatures in short-term experiments, which is consistent with our quantitative RT-PCR experiment where the transcription of CrFAD7 was repressed at a higher cultivation temperature. Such an increased resistance of the PSII activity to high-temperature stress in a desaturase mutant has been previously observed in the *Arabidopsis fad3fad7fad8* triple mutant (Routaboul et al., 2012) and has also been reported for another *C. reinhardtii* mutant, *hf-9*, probably deficient in  $\omega$ -6 desaturation (Sato et al., 1995, 1996). One of the possible explanations for this phenomenon could be that PUFAs, major components of photosynthetic membranes, are prone to oxidation (Frankel, 1991). Under high-temperature stress, oxidation of the plastidial membrane lipids containing high levels of  $\omega$ -3 fatty acids (as in the wild type) might occur at a faster rate than in strains containing low amount of  $\omega$ -3 fatty

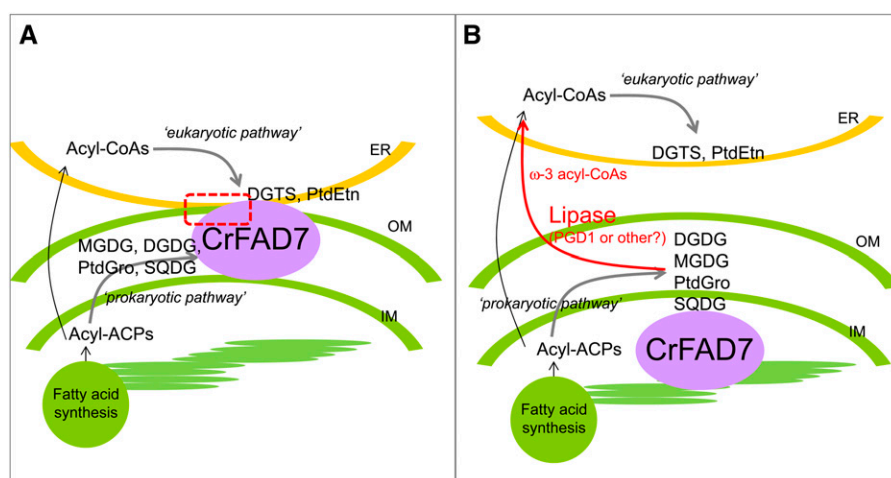


**Figure 10.** Possible models involving the plastidial CrFAD7 for the desaturation of  $\omega$ -3 fatty acids present in extraplastidic membrane lipids. A, CrFAD7 acts on the plastid envelope at plastid-ER contact sites (red dashed area). B, The  $\omega$ -3 fatty acids are synthesized in the plastid, clipped off the plastidic lipids through a specific lipase(s), and exported out into the ER as acyl-CoAs via the classical route for 16:0/18:0/18:1. ACP, Acyl carrier protein; IM, inner plastid envelope; OM, outer plastid envelope. [See online article for color version of this figure.]

acids (*crfad7*), thus resulting in the loss of PSII activities sooner.

Through the generation of a zero “ $\omega$ -3 fatty acid” mutant in *Arabidopsis* (Routaboul et al., 2000) as well as in the cyanobacterium *Synechococcus* sp. PCC7002 (Sakamoto et al., 1998), it has been demonstrated that  $\omega$ -3 fatty acids are required for continuous cell growth at low temperatures. In this study, no difference in cell growth was observed between the wild type and the *C. reinhardtii* mutant *crfad7* when they were cultivated at 15°C. The lack of a cold-sensitivity phenotype in *crfad7* might be partly due to the fact that *crfad7* is a knock-down mutant, not a knockout mutant, and that the increased  $\omega$ -6 trienoic acids [C16:3(4,7,10) and C18:3(5,9,12); Fig. 1] in *crfad7* may functionally replace the missing  $\omega$ -3 fatty acids. It could also be that *C. reinhardtii* resembles the cyanobacterium *Synechocystis* sp. PCC6803, where mutants of this cyanobacterium with considerable amounts of dienoic acids grew the same as the wild type at lower temperatures and a suppressed growth was observed only in cells where all PUFAs (dienoic and trienoic) were replaced by monounsaturated or saturated fatty acids (Tasaka et al., 1996). This and other explanations could only be verified in the future with the isolation of null mutant(s) of  $\omega$ -3 fatty acids in *C. reinhardtii*.

## CONCLUSION

*crfad7* is one of the first series of mutants we have isolated from a large-scale forward genetic screen. From detailed characterization of this mutant, we provide experimental evidence that *C. reinhardtii* contains only a single  $\omega$ -3 FAD, CrFAD7. From a biotechnological point of view, the molecular identification and characterization of the *CrFAD7* gene provides tools to modify the fatty acid compositions of algal oils for improved nutrition, biofuel, and other purposes.

## MATERIALS AND METHODS

### Strains and Culture Conditions

The wild-type strain 137C (*mt<sup>-</sup> nit1 nit2*) was used for generating the insertional mutant library. Unless otherwise stated, *Chlamydomonas reinhardtii* cells were grown in shake flasks at 25°C under continuous illumination (100  $\mu$ mol photons  $m^{-2} s^{-1}$ ) in Tris-acetate phosphate (TAP) medium (i.e. mixotrophic condition; Harris, 2001). For all experiments, cells were cultivated in TAP medium until the exponential phase (about  $2 \times 10^6$  to  $6 \times 10^6$  cells  $mL^{-1}$ ) and diluted a couple of times in fresh medium before being used for experiments. Cell concentration and cell size (cellular volume and diameter) were monitored using an automated cell counter (Multisizer 3 Coulter Counter; Beckman Coulter). Growth kinetics was also followed by measuring the optical density at 750 nm using a spectrophotometer (Schimadzu UV-260).

For mutant screening, individual *C. reinhardtii* colonies were inoculated into 3 mL of TAP medium in a 12-mL sterile plastic tube. Earlier stationary-grown cells were harvested by centrifugation at 1,800g for 10 min at 4°C. The cell pellets were subjected to fatty acid composition analysis as detailed below.

### Nuclear Transformation and Generation of a Mutant Library for *C. reinhardtii*

An insertional mutant library was generated by transformation of the *aphVIII* cassette into the wild-type strain 137C. A fragment (1.8 kb) containing

the *aphVIII* gene and its promoter *HSP70A/RBCS2* (Sizova et al., 2001) was gel purified after digesting the pSL18 vector (kindly provided by Prof. Steven Ball, University of Lille) with *KpnI* and *XhoI*. The method of nuclear transformation by electroporation (Shimogawara et al., 1998) was used with slight modifications. Exponential phase-grown cells were harvested by centrifugation at 360g for 3 min at room temperature. Cell pellets were resuspended in home-made autolysin (prepared as described by Harris, 2009) and incubated at room temperature for 2 h under gentle shaking and low-light conditions. Autolysin treatment removed cell wall and thus facilitated foreign DNA penetration. After autolysin treatment, cells were collected by centrifugation and resuspended in TAP medium containing 40 mM Suc to a concentration of  $3 \times 10^8$  cells  $mL^{-1}$ . For each transformation, 0.5  $\mu$ g of the DNA fragment containing the *aphVIII* gene was mixed with  $1 \times 10^8$  cells and placed into an electroporation cuvette with a 2-mm gap (Bio-Rad Laboratories). An electric pulse of 750 V was applied to the mixture for 5 ms. The cells were then mixed gently with 1 mL of TAP medium containing 20% (w/v) cornstarch and 40 mM Suc before being spread onto a TAP agar plate containing 10  $\mu$ g  $mL^{-1}$  paromomycin for selection. Colonies resistant to paromomycin can be seen after around 10 d of cultivation.

### DNA Extraction and Vector Construction

Total DNA was extracted from exponential-grown cells of *C. reinhardtii* following the protocol described before (Tolletier et al., 2011).

### For Nuclear Complementation

The genomic region containing the *CrFAD7* gene (Phytozome Cre01.g038600) was amplified using the primers *NdeI-FAD7-F* and *EcoRV-FAD7-R* (all primer sequences used in this study are presented in Supplemental Table S3). The amplified gene was cloned as an *NdeI-EcoRV* fragment into the vector pSL-hyg, which contains the *aphVII* gene conferring hygromycin resistance (Berthold et al., 2002). The resulting construct was transformed into the mutant (*crfad7*) background, resulting in transformants named *crfad7:nuCrFAD7* (where *nu* = nuclear). Transformed cells were initially selected on TAP agar plates containing 10  $\mu$ g  $mL^{-1}$  hygromycin, and complemented lines were selected based on fatty acid composition analysis.

### For Protein Subcellular Localization

The 3xHA tag was amplified from the vector p3xHA (purchased from the *Chlamydomonas* Resource Center) using primers *inF HA Fw* and *inF HA Rev*. The amplification was done using Phusion High Fidelity polymerases (Finnzymes). The PCR product was introduced to the *XbaI*-linearized pSL-hyg, digested by *EcoRV*, using the In-Fusion HD Cloning Kit (Clontech) to make the vector pSL-hyg-HA. The genomic DNA sequence encoding *CrFAD7* was amplified using primers *InF FAD7 Fw* and *InF FAD7 Rev*. Amplified *CrFAD7* was then integrated into pSL-hyg-HA using the In-Fusion HD Cloning Kit to make a C-terminal fusion to HA. This construct (pSL-hyg-nuCrFAD7-HA) was inserted into the nuclear genome of the *crfad7* mutant. Transformed cells were first selected on TAP agar plates containing 10  $\mu$ g  $mL^{-1}$  hygromycin.

### For Plastid Transformation

To ensure a high and stable gene expression in the plastid genome of *C. reinhardtii*, a synthetic gene corresponding to the coding sequence of *CrFAD7* and based on the codon usage of plastid-encoded genes was designed and synthesized by GeneArt (Life Technologies). The GC content of the synthetic gene is 35% compared with 65% in the native *CrFAD7* gene (Phytozome Cre01.g038600). The synthetic gene was cloned downstream of a *psaA* promoter into the vector pLM20 (Michelet et al., 2011) harboring an *aadA* gene conferring resistance to spectinomycin. The vector pLM20 was kindly provided by Dr. Michel Goldschmidt-Clermont (University of Geneva). The resulting transformed lines were named *crfad7:cpCrFAD7* (where *cp* is chloroplast).

### RNA Extraction and Quantitative RT-PCR

RNA was extracted from exponential-grown cells following the protocol of Mus et al. (2007). Briefly, cells of *C. reinhardtii* were harvested by centrifugation and then immediately frozen in liquid nitrogen. To the cell pellet, 0.5 mL of Plant RNA Reagent (Life Technologies) was added, and cells were

resuspended by pipetting and transferred into 2-mL prefilled tubes with ceramic beads (Bertin Technologies). The cell suspension was then homogenized via a twice 10-s vortex in a homogenizer at 5,500 rpm (Precellys 24; Bertin Technologies) at 4°C. The tubes were then centrifuged at 13,000g for 2 min at room temperature, and the supernatant was transferred to DNase/RNase-free tubes. To these tubes, NaCl (0.1 mL, 5 M) and chloroform were added sequentially. These tubes were mixed and then centrifuged at 13,000g for 10 min at 4°C. The upper aqueous phase was transferred to new tubes, to which an equal volume of isopropanol was added, mixed, and centrifuged again at 13,000g for 10 min at 4°C. After gently decanting the supernatant, 0.5 mL of 70% (v/v) ethanol was added to wash the pellet. After centrifugation, the pellet was air dried, and then RNA was dissolved in DNase/RNase-free water. Contaminating DNA was eliminated by DNase treatment (Ambion, Invitrogen), and RNA was purified with Nucleospin RNA Clean Up (Macherey Nagel). Extracted RNA was quantified using a spectrophotometer (NanoDrop 2000c; Thermo Scientific).

The RT reaction was done on 1  $\mu$ g of total RNA using the SuperScript Vilo cDNA Synthesis Kit (Life Technologies) as described by the manufacturer. The primers used were *fad7 F*, *fad7 R*, *rack1 F*, and *rack1 R* with a product between 50 and 150 bp. Quantitative RT-PCR was performed on 384-well plates using the LightCycler 480 instrument (Roche), and reactions were done with MESA FAST qPCR MasterMix Plus for SYBR Assay No ROX (Eurogentec). The cycling conditions used were as follows: 95°C for 10 min, then 45 cycles at 95°C for 10 s, 60°C for 15 s, and 72°C for 10 s. The relative transcript ratio of *CrFAD7* was calculated based on the  $2^{-\Delta\Delta CT}$  method (Livak and Schmittgen, 2001), with average cycle threshold obtained based on triplicate measurements. Relative expression ratios were calculated based on three independent experiments. The *rack1* (locus g6364) gene encoding the protein receptor for activated protein kinase C was used as a housekeeping gene for normalization, as reported previously for *C. reinhardtii* (Mus et al., 2007).

## Plastid Transformation

Chloroplast transformation of *C. reinhardtii* using gene gun bombardment has been described previously (Boynton et al., 1988). Briefly, the *crfad7* mutant was cultivated in TAP medium until midlog phase, harvested by gentle centrifugation, and then resuspended in TAP medium to a final concentration of  $1.5 \times 10^8$  cells mL<sup>-1</sup>. The cell suspension (150  $\mu$ L) was spread onto a TAP agar plate supplemented with 100  $\mu$ g mL<sup>-1</sup> spectinomycin (Michelet et al., 2011), and the plates were bombarded with gold particles (S550d; Seashell Technology) coated with the plasmid pLM20-*cpCrFAD7* (helium gun; velocity of 7 bar). The plates were then placed at 25°C under standard light conditions for cell propagation and selection.

## Lipid Extraction, Quantification by High-Performance TLC, and FAME Analysis

The procedures to extract lipids and analyze them by TLC or GC have been described in detail elsewhere (Siaut et al., 2011). Briefly, a modified method of Bligh and Dyer (1959) was used to extract *C. reinhardtii* lipids. Each lipid class was quantified after separation by TLC using a densitometry method by comparing with a curve generated from a known amount of lipid standard for each class, with the exception of DGTS, which is calculated based on PtdCho, since no commercial DGTS is available. FAMES are prepared from extracted lipids or directly from *C. reinhardtii* cell pellets based on a modified acid-catalyzed transmethylation method (Li et al., 2006). FAMES were analyzed by GC-FID.

## Lipid Molecular Species Analysis by UPLC-MS/MS

For lipidomic analysis, harvested cells were immediately boiled in hot isopropanol for 10 min at 85°C to quench lipase activities, thus minimizing the potential degradation of lipids. The hexane-hot isopropanol method described by Hara and Radin (1978) was used. After cooling down, quenched cells were vortexed for 10 min to break the cells. Hexane was added to reach a final ratio of water:isopropanol:hexane of 1:4:6 (v/v/v) and vortexed again. An aqueous Na<sub>2</sub>SO<sub>4</sub> solution (6.6%, w/v) was added to allow phase separation. After centrifugation, the upper phase was collected and transferred to a new glass tube. A mixture of isopropanol:hexane (2:7, v/v) was used to reextract the lipids. The upper hexane phase was pooled with the previous organic extracts, then samples were dried under N<sub>2</sub> flow and resuspended in methanol:CHCl<sub>3</sub> (1:2, v/v) for UPLC-MS/MS analysis.

## Annotation of Lipid Species

Lipid species were annotated by molecular composition as described previously (Ejsing et al., 2009): lipid class(carbon number in the first fatty acid: number of unsaturations in the first fatty acid – carbon number in the second fatty acid:number of unsaturations in the second fatty acid). For example, for a PtdEtn molecule with C16:0 and C18:3 fatty acids, it is written as PtdEtn(16:0-18:3). It is worth noting that this annotation does not distinguish the stereospecific position of each fatty acid on the glycerol backbone.

## Liquid Chromatography Separation

Lipid extracts were separated on a Kinetex C<sub>18</sub> column (diameter 2.6  $\mu$ m, 2.1  $\times$  150 mm; Phenomenex) connected to an Ultimate RS3000 UPLC system (Thermo Scientific). A binary solvent system was used, in which mobile phase A consisted of acetonitrile:water (60:40, v/v) and 10 mM ammonium formate and mobile phase B consisted of isopropanol:acetonitrile (90:10, v/v), 10 mM ammonium formate, and 0.1% formic acid (v/v). Separations were done over a 32-min period following the conditions described before (Hu et al., 2008a). A flow rate of 300  $\mu$ L min<sup>-1</sup> was used for the analysis. Column and sample trays were held at 45°C and 7°C, respectively. The same buffer conditions were used for all experiments.

## Mass Spectrometry

The UPLC system was coupled to a Triple TOF 5600 mass spectrometer (ABSciex) equipped with a duo-spray ion source. The UPLC device and the calibration pump were connected, respectively, to the electrospray ionization probe and the atmospheric pressure chemical ionization probe. Source parameters included nebulizing gases GS1 at 40, GS2 at 60, curtain at 20, positive mode ion spray voltage at 5,500, negative mode ion spray voltage at -5,500, declustering potential at 40 V, and an electrospray ionization source operating temperature of 500°C. The instrument was tuned every six runs by a calibrated pump that delivers mass calibration solution of both positive and negative mode for mass spectrometry and MS/MS.

## Lipid Species Identification

Data were acquired in an information-dependent acquisition experiment containing a survey scan covering a mass range of 400 to 1,100 mass-to-charge ratio and several corresponding product-ion scans at different collision energies (collision energy set to 40 and collision energy spread set to 25). Different information-dependent acquisition criteria are a mass tolerance for candidate ions of 50 mD, a maximum number of ions to monitor per cycle set to 14, a previously selected target ion excluded for 30 s, and exclude isotope within set to 2. The data were analyzed with Analyst Software (Applied Biosystems). Lipid identification is based on retention time, mass accuracy peaks from the mass spectrometry survey scan compared with theoretical masses, and fragment ions from the MS/MS scan. Polar membrane lipids MGDG, DGDG, DGTS, PtdEtn, phosphatidylglycerol, and SQDG were analyzed in negative ionization mode, while triglycerides (e.g. TAGs) were analyzed by positive ionization mode. For fatty acyl group identification, a given lipid ion was selected as precursor ion and then subjected to collision energy (46 V). The fatty acyl groups were identified based on the fragments deriving from the neutral loss of individual acyl groups.

## Lipid Species Quantification

Relative quantification is achieved with Multiquant software (Applied Biosystems) on the basis of intensity values of extracting masses of different lipids identified previously. Due to differences in ionization efficiency between polar components (i.e. different lipid classes), in this study, we have taken a comparative lipidomic approach rather than absolute quantification of each lipid. Since the amount of total fatty acids per cell is constant between the wild type, the mutant *crfad7*, and two complemented lines, total lipids were extracted and one aliquot was subjected to total FAME analyses allowing fatty acid quantification. Based on this, the other aliquot was diluted to reach a final concentration of 100 ng FAME  $\mu$ L<sup>-1</sup>, 0.2  $\mu$ L of which was injected for UPLC-MS/MS. The injection is based on equal loading of total FAMES for all four strains compared.

## Protein Extraction and Western Blotting

*C. reinhardtii* cells were harvested and resuspended in Tricine-KOH buffer (50 mM, pH 8.0) containing 150 mM NaCl and a protease inhibitor cocktail for plant cells (Sigma-Aldrich). Cells were lysed by sonication. Soluble and

membrane proteins were separated by centrifuging the cell suspension at 9,300g for 10 min. Cold acetone and 10% SDS (w/v) were added to the cell suspension to help precipitate proteins. Protein concentration was determined using the bicinchoninic acid protein assay reagent (Thermo Scientific).

For western blotting, the protein pellet was resuspended in denaturing blue NuPage (Invitrogen) and denatured at 95°C for 10 min. For each lane, approximately 15 µg of proteins was loaded on a 10% SDS-PAGE gel. After migration at 150 V in Tris-Glyc buffer, the proteins were then transferred to a nitrocellulose membrane. Standard antibody hybridization procedure was carried out in Tris-buffered saline-Tween buffer containing affinity-purified rabbit anti-HA primary antibodies or secondary antibodies conjugated to the anti-rabbit IgG-fluorescein isothiocyanate (FITC). The concentration of each antibody was applied as indicated by the manufacturer. Chemiluminescent signal was revealed using disodium 3-(4-methoxyphosphoryl)-1,2-dioxetane-3,2'-(5'-chloro)tricyclo[3.3.1.1<sup>3,7</sup>]decan-4-yl)phenyl phosphate (Roche; product no. 11755633001) and photographed in a G:Box (Syngene).

### Subcellular Localization of CrFAD7 Based on Immunofluorescence

For hybridization and microscopic observation, the protocol of Cole et al. (1998) was used with some modifications. Briefly, exponential-grown *C. reinhardtii* cells were placed on a Poly-Prep slide (Sigma) for 10 min, and extra culture medium was removed using a Pasteur pipette. The slide was then dipped in cold methanol (−20°C) for 2 min, followed by rinsing five times with phosphate-buffered saline (PBS) before being blocked with PBS containing 1% bovine serum albumin for 30 min. The cells were washed five times again with PBS and then incubated for 2 h with PBS containing 1% bovine serum albumin and anti-HA antibodies (primary antibodies; Sigma H6908). Cells were washed a final time with PBS before incubation with the anti-rabbit IgG-FITC (secondary antibodies; Sigma F4890) for 1 h. Slides were washed five times with PBS before being mounted with Prolong Gold antifade reagent (Invitrogen). Stained cells were observed with a confocal laser scanning microscope (Leica SP2) after excitation under the laser line 488 nm. Emission signals were collected at 498 to 515 nm and 656 to 714 nm for FITC and chlorophyll autofluorescence, respectively.

### Temperature Stress Experiments and Measurement of Photosynthetic Activity of PSII

For the measurement of photosynthetic activities, cells of *C. reinhardtii* were grown in photoautotrophic conditions with supply of 2% CO<sub>2</sub> (i.e. replacing acetic acid in regular TAP medium by hydrochloric acid; Chochois et al., 2010). To test heat stress, midlog phase-grown cells at 25°C were transferred into 15°C, 25°C, and 45°C. To measure the PSII activity using a Dual Pam 100 (Heinz Walz), culture of *C. reinhardtii* (1.5 mL) was placed into a cuvette under stirring at room temperature for 30 min in the dark. Actinic light was increased stepwise from 3 to 960 µmol photons m<sup>−2</sup> s<sup>−1</sup>. After 30 s under each given light regime, a saturating flash (10,000 µmol photons m<sup>−2</sup> s<sup>−1</sup>; 200-ms duration) was supplied to measure maximal fluorescence ( $F_m$ ). The ratio of variable fluorescence ( $F_v$ ) to maximal fluorescence ( $F_m$ ) indicates the maximum quantum efficiency.  $F_v/F_m$  is calculated based on the following equation:  $F_v/F_m = (F_m - F_o)/F_m$  (Genty et al., 1989).

### Bioinformatic Analyses

To identify homologs of FAD7 in Chlorophyceae microalgae with sequenced genomes, we used CrFAD7 (locus Cre01.g038600) as bait and employed the BLASTP program (BLASTP 2.2.26+) hosted at Phytozome version 9.1 (<http://www.phytozome.net/>) or the Genome Portal hosted at the Joint Genome Institute (<http://genome.jgi-psf.org/>). The default settings were used. Protein subcellular localization is predicted by the PredAlgo program (Tardif et al., 2012), which is freely available online at <https://giavap-genomes.ibpc.fr/cgi-bin/predalgotdb.perl?page=main>.

The accession numbers used in this study are as follows: Cre01.g038600 (CrFAD7), g6364 (RACK1), sl11441 (DesB), At3g11170 (AtFAD7), At2g29980 (AtFAD3), and At5g05580 (AtFAD8).

### Supplemental Data

The following materials are available in the online version of this article.

**Supplemental Figure S1.** Fatty acid compositions (mol %) for individual lipid classes after being separated by TLC.

**Supplemental Figure S2.** Comparison of TAG content between the wild type and the mutant *crfad7* under standard growth conditions and nitrogen starvation for 48 h.

**Supplemental Figure S3.** Analysis of the number of *aphVIII* insertions and linkage between altered fatty acid phenotype and paromomycin resistance.

**Supplemental Figure S4.** Quantitative RT-PCR analyses of the transcription level of *CrFAD7* in the wild type, the mutant *crfad7*, and four nuclear complemented lines.

**Supplemental Figure S5.** FAME analyses of several complemented lines of the mutant *crfad7* by plastidial transformation of a codon-adapted *CrFAD7* gene.

**Supplemental Figure S6.** Proportions (mol %) of fatty acids in the wild type and the mutant *crfad7* when cultivated at a temperature of 15°C.

**Supplemental Figure S7.** Comparison of cell size, growth kinetics, and chlorophyll content between the wild type, *crfad7*, and the two complemented lines (*crfad7::nuCrFAD7* and *crfad7::cpCrFAD7*).

**Supplemental Figure S8.** Fatty acid compositions remain constant during short-term heat stress (45°C) for both the wild type and *crfad7*, but the difference between the wild type and *crfad7* remain constant at elevated temperatures.

**Supplemental Table S1.** Comparison of polar membrane lipid molecular species present in WT and *crfad7* by LC-MS/MS (same data set and legend as presented in Fig. 7).

**Supplemental Table S2.** Phylogenetic analysis of FAD in oxygenic photosynthetic organisms.

**Supplemental Table S3.** Names and sequences of the primers used in this study.

**Supplemental Text S1.** Supplemental Materials and Methods.

### ACKNOWLEDGMENTS

We are grateful to Dr. Miriam Schulz-Raffelt for her advice during the immunohybridization procedure, to Dr. H el ene Javot for her advice on confocal microscopy, to Jean-Marc Adriano for his guidance on western blots, and to Anthony Baltz for his help with plastid transformation. We also thank Patrick Carrier and R emy Puppo for their technical assistance.

Received July 2, 2013; accepted August 16, 2013; published August 19, 2013.

### LITERATURE CITED

- Andersson MX, Goks or M, Sandelius AS (2007) Optical manipulation reveals strong attracting forces at membrane contact sites between endoplasmic reticulum and chloroplasts. *J Biol Chem* **282**: 1170–1174
- Andreu V, Collados R, Testillano PS, Risue o MdC, Picorel R, Alfonso M (2007) In situ molecular identification of the plastid  $\omega$ 3 fatty acid desaturase FAD7 from soybean: evidence of thylakoid membrane localization. *Plant Physiol* **145**: 1336–1344
- Aronel V, Lemieux B, Hwang J, Gibson S, Goodman HM, Somerville CR (1992) Map-based cloning of a gene controlling omega-3 fatty acid desaturation in Arabidopsis. *Science* **258**: 1353–1355
- Beer LL, Boyd ES, Peters JW, Posewitz MC (2009) Engineering algae for biohydrogen and biofuel production. *Curr Opin Biotechnol* **20**: 264–271
- Berthold P, Schmitt R, Mages W (2002) An engineered *Streptomyces hygroscopicus* aph 7'' gene mediates dominant resistance against hygromycin B in *Chlamydomonas reinhardtii*. *Protist* **153**: 401–412
- Bligh EG, Dyer WJ (1959) A rapid method of total lipid extraction and purification. *Can J Biochem Physiol* **37**: 911–917
- Boyle NR, Page MD, Liu B, Blaby IK, Casero D, Kropat J, Cokus SJ, Hong-Hermesdorf A, Shaw J, Karpowicz SJ, et al (2012) Three acyltransferases and nitrogen-responsive regulator are implicated in nitrogen starvation-induced triacylglycerol accumulation in *Chlamydomonas*. *J Biol Chem* **287**: 15811–15825

- Boynton JE, Gillham NW, Harris EH, Hosler JP, Johnson AM, Jones AR, Randolph-Anderson BL, Robertson D, Klein TM, Shark KB, et al (1988) Chloroplast transformation in *Chlamydomonas* with high velocity microprojectiles. *Science* **240**: 1534–1538
- Browse J, McCourt P, Somerville C (1986a) A mutant of *Arabidopsis* deficient in c(18:3) and c(16:3) leaf lipids. *Plant Physiol* **81**: 859–864
- Browse J, Warwick N, Somerville CR, Slack CR (1986b) Fluxes through the prokaryotic and eukaryotic pathways of lipid synthesis in the '16:3' plant *Arabidopsis thaliana*. *Biochem J* **235**: 25–31
- Chi XY, Zhang XW, Guan XY, Ding L, Li YX, Wang MQ, Lin HZ, Qin S (2008) Fatty acid biosynthesis in eukaryotic photosynthetic microalgae: identification of a microsomal delta 12 desaturase in *Chlamydomonas reinhardtii*. *J Microbiol* **46**: 189–201
- Chochois V, Constans L, Dauvillee D, Beyly A, Soliveres M, Ball S, Peltier G, Cournac L (2010) Relationships between PSII-independent hydrogen bioproduction and starch metabolism as evidenced from isolation of starch catabolism mutants in the green alga *Chlamydomonas reinhardtii*. *Int J Hydrogen Energy* **35**: 10731–10740
- Cole DG, Diener DR, Himelblau AL, Beech PL, Fuster JC, Rosenbaum JL (1998) *Chlamydomonas* kinesin-II-dependent intraflagellar transport (IFT): IFT particles contain proteins required for ciliary assembly in *Caenorhabditis elegans* sensory neurons. *J Cell Biol* **141**: 993–1008
- Day A, Rochaix JD (1991) A transposon with an unusual LTR arrangement from *Chlamydomonas reinhardtii* contains an internal tandem array of 76 bp repeats. *Nucleic Acids Res* **19**: 1259–1266
- Day A, Schirmer-Rahire M, Kuchka MR, Mayfield SP, Rochaix JD (1988) A transposon with an unusual arrangement of long terminal repeats in the green alga *Chlamydomonas reinhardtii*. *EMBO J* **7**: 1917–1927
- Dyer JM, Mullen RT (2001) Immunocytological localization of two plant fatty acid desaturases in the endoplasmic reticulum. *FEBS Lett* **494**: 44–47
- Ejsing CS, Sampaio JL, Surendranath V, Duchoslav E, Ekroos K, Klemm RW, Simons K, Shevchenko A (2009) Global analysis of the yeast lipidome by quantitative shotgun mass spectrometry. *Proc Natl Acad Sci USA* **106**: 2136–2141
- Fan JL, Andre C, Xu CC (2011) A chloroplast pathway for the *de novo* biosynthesis of triacylglycerol in *Chlamydomonas reinhardtii*. *FEBS Lett* **585**: 1985–1991
- Frankel EN (1991) Recent advances in lipid oxidation. *J Sci Food Agric* **54**: 495–511
- Genty B, Briantais JM, Baker NR (1989) The relationship between the quantum yield of photosynthetic electron-transport and quenching of chlorophyll fluorescence. *Biochim Biophys Acta* **990**: 87–92
- Giroud C, Eichenberger W (1988) Fatty acids of *Chlamydomonas reinhardtii*: structure, positional distribution and biosynthesis. *Biol Chem Hoppe Seyler* **369**: 18–19
- Giroud C, Eichenberger W (1989) Lipids of *Chlamydomonas reinhardtii*: incorporation of C-14 acetate, C-14 palmitate and C-14 oleate into different lipids and evidence for lipid-linked desaturation of fatty acids. *Plant Cell Physiol* **30**: 121–128
- Giroud C, Gerber A, Eichenberger W (1988) Lipids of *Chlamydomonas reinhardtii*: analysis of molecular species and intracellular sites of biosynthesis. *Plant Cell Physiol* **29**: 587–595
- Goodson C, Roth R, Wang ZT, Goodenough U (2011) Structural correlates of cytoplasmic and chloroplast lipid body synthesis in *Chlamydomonas reinhardtii* and stimulation of lipid body production with acetate boost. *Eukaryot Cell* **10**: 1592–1606
- Guschina IA, Harwood JL (2006) Lipids and lipid metabolism in eukaryotic algae. *Prog Lipid Res* **45**: 160–186
- Hara A, Radin NS (1978) Lipid extraction of tissues with a low-toxicity solvent. *Anal Biochem* **90**: 420–426
- Harris EH (2001) *Chlamydomonas* as a model organism. *Annu Rev Plant Physiol Plant Mol Biol* **52**: 363–406
- Harris EH (2009) *The Chlamydomonas Sourcebook: Introduction to Chlamydomonas and Its Laboratory Use*, Ed 2. Elsevier, Oxford.
- Harwood JL, Guschina IA (2009) The versatility of algae and their lipid metabolism. *Biochimie* **91**: 679–684
- Hu C, van Dommelen J, van der Heijden R, Spijksma G, Reijmers TH, Wang M, Sleen E, Lu X, Xu G, van der Greef J, et al (2008a) RPLC-ion-trap-FTMS method for lipid profiling of plasma: method validation and application to p53 mutant mouse model. *J Proteome Res* **7**: 4982–4991
- Hu Q, Sommerfeld M, Jarvis E, Ghirardi M, Posewitz M, Seibert M, Darzins A (2008b) Microalgal triacylglycerols as feedstocks for biofuel production: perspectives and advances. *Plant J* **54**: 621–639
- Jouhet J, Maréchal E, Block MA (2007) Glycerolipid transfer for the building of membranes in plant cells. *Prog Lipid Res* **46**: 37–55
- Joyard J, Teyssier E, Miege C, Beryn-Seigneurin D, Marechal E, Block MA, Dorne AJ, Rolland N, Ajlani G, Douce R (1998) The biochemical machinery of plastid envelope membranes. *Plant Physiol* **118**: 715–723
- Kajikawa M, Yamato KT, Kohzu Y, Shoji S, Matsui K, Tanaka Y, Sakai Y, Fukuzawa H (2006) A front-end desaturase from *Chlamydomonas reinhardtii* produces pinolenic and coniferonic acids by omega13 desaturation in methylotrophic yeast and tobacco. *Plant Cell Physiol* **47**: 64–73
- Khazin-Goldberg I, Iskandarov U, Cohen Z (2011) LC-PUFA from photosynthetic microalgae: occurrence, biosynthesis, and prospects in biotechnology. *Appl Microbiol Biotechnol* **91**: 905–915
- Kis M, Zsiros O, Farkas T, Wada H, Nagy F, Gombos Z (1998) Light-induced expression of fatty acid desaturase genes. *Proc Natl Acad Sci USA* **95**: 4209–4214
- Krogh A, Larsson B, von Heijne G, Sonnhammer EL (2001) Predicting transmembrane protein topology with a hidden Markov model: application to complete genomes. *J Mol Biol* **305**: 567–580
- Lechtreck KF, Luro S, Awata J, Witman GB (2009) HA-tagging of putative flagellar proteins in *Chlamydomonas reinhardtii* identifies a novel protein of intraflagellar transport complex B. *Cell Motil Cytoskeleton* **66**: 469–482
- Li X, Moellering ER, Liu B, Johnny C, Fedewa M, Sears BB, Kuo MH, Benning C (2012a) A galactoglycerolipid lipase is required for triacylglycerol accumulation and survival following nitrogen deprivation in *Chlamydomonas reinhardtii*. *Plant Cell* **24**: 4670–4686
- Li XB, Benning C, Kuo MH (2012b) Rapid triacylglycerol turnover in *Chlamydomonas reinhardtii* requires a lipase with broad substrate specificity. *Eukaryot Cell* **11**: 1451–1462
- Li YH, Beisson F, Pollard M, Ohlrogge J (2006) Oil content of *Arabidopsis* seeds: the influence of seed anatomy, light and plant-to-plant variation. *Phytochemistry* **67**: 904–915
- Li-Beisson Y, Shorrosh B, Beisson F, Andersson MX, Arondel V, Bates PD, Baud S, Bird D, DeBono A, Durrett TP, et al (2010) Acyl-lipid metabolism. *The Arabidopsis Book* **8**: e0999, doi/10.1199/tab.0999
- Liu B, Benning C (2013) Lipid metabolism in microalgae distinguishes itself. *Curr Opin Biotechnol* **24**: 300–309
- Livak KJ, Schmittgen TD (2001) Analysis of relative gene expression data using real-time quantitative PCR and the 2(- $\Delta\Delta C(T)$ ) method. *Methods* **25**: 402–408
- Los DA, Murata N (1998) Structure and expression of fatty acid desaturases. *Biochim Biophys Acta* **1394**: 3–15
- McCann M, Hugly S, Browse J, Somerville C (1994) A mutation at the *fad8* locus of *Arabidopsis* identifies a second chloroplast  $\omega$ -3 desaturase. *Plant Physiol* **106**: 1609–1614
- Mendiola-Morgenthaler L, Eichenberger W, Boschetti A (1985) Isolation of chloroplast envelopes from *Chlamydomonas*: lipid and polypeptide composition. *Plant Sci* **41**: 97–104
- Merchant SS, Kropat J, Liu B, Shaw J, Warakanont J (2012) TAG, you're it! *Chlamydomonas* as a reference organism for understanding algal triacylglycerol accumulation. *Curr Opin Biotechnol* **23**: 352–363
- Merchant SS, Prochnik SE, Vallon O, Harris EH, Karpowicz SJ, Witman GB, Terry A, Salamov A, Fritz-Laylin LK, Maréchal-Drouard L, et al (2007) The *Chlamydomonas* genome reveals the evolution of key animal and plant functions. *Science* **318**: 245–250
- Michele L, Lefebvre-Legendre L, Burr SE, Rochaix JD, Goldschmidt-Clermont M (2011) Enhanced chloroplast transgene expression in a nuclear mutant of *Chlamydomonas*. *Plant Biotechnol J* **9**: 565–574
- Miquel M, Browse J (1992) *Arabidopsis* mutants deficient in polyunsaturated fatty acid synthesis: biochemical and genetic characterization of a plant oleoyl-phosphatidylcholine desaturase. *J Biol Chem* **267**: 1502–1509
- Mus F, Dubini A, Seibert M, Posewitz MC, Grossman AR (2007) Anaerobic acclimation in *Chlamydomonas reinhardtii*: anoxic gene expression, hydrogenase induction, and metabolic pathways. *J Biol Chem* **282**: 25475–25486
- Mustardy L, Los DA, Gombos Z, Murata N (1996) Immunocytochemical localization of acyl-lipid desaturases in cyanobacterial cells: evidence that both thylakoid membranes and cytoplasmic membranes are sites of lipid desaturation. *Proc Natl Acad Sci USA* **93**: 10524–10527
- Nakamura MT, Nara TY (2004) Structure, function, and dietary regulation of delta6, delta5, and delta9 desaturases. *Annu Rev Nutr* **24**: 345–376
- Napier JA, Michaelson LV, Stobart AK (1999) Plant desaturases: harvesting the fat of the land. *Curr Opin Plant Biol* **2**: 123–127
- Radakovits R, Jinkerson RE, Darzins A, Posewitz MC (2010) Genetic engineering of algae for enhanced biofuel production. *Eukaryot Cell* **9**: 486–501

- Reyes-Prieto A, Weber APM, Bhattacharya D** (2007) The origin and establishment of the plastid in algae and plants. *Annu Rev Genet* **41**: 147–168
- Riekhof WR, Sears BB, Benning C** (2005) Annotation of genes involved in glycerolipid biosynthesis in *Chlamydomonas reinhardtii*: discovery of the betaine lipid synthase BTA1Cr. *Eukaryot Cell* **4**: 242–252
- Rolland N, Curien G, Finazzi G, Kuntz M, Maréchal E, Matringe M, Ravanel S, Seigneurin-Berny D** (2012) The biosynthetic capacities of the plastids and integration between cytoplasmic and chloroplast processes. *Annu Rev Genet* **46**: 233–264
- Rosenberg JN, Oyler GA, Wilkinson L, Betenbaugh MJ** (2008) A green light for engineered algae: redirecting metabolism to fuel a biotechnology revolution. *Curr Opin Biotechnol* **19**: 430–436
- Routaboul JM, Fischer SF, Browse J** (2000) Trienoic fatty acids are required to maintain chloroplast function at low temperatures. *Plant Physiol* **124**: 1697–1705
- Routaboul JM, Skidmore C, Wallis JG, Browse J** (2012) *Arabidopsis* mutants reveal that short- and long-term thermotolerance have different requirements for trienoic fatty acids. *J Exp Bot* **63**: 1435–1443
- Sakamoto T, Shen GZ, Higashi S, Murata N, Bryant DA** (1998) Alteration of low-temperature susceptibility of the cyanobacterium *Synechococcus* sp. PCC 7002 by genetic manipulation of membrane lipid unsaturation. *Arch Microbiol* **169**: 20–28
- Sato N, Sonoike K, Kawaguchi A, Tsuzuki M** (1996) Contribution of lowered unsaturation levels of chloroplast lipids to high temperature tolerance of photosynthesis in *Chlamydomonas reinhardtii*. *J Photochem Photobiol B* **36**: 333–337
- Sato N, Tsuzuki M, Matsuda Y, Ehara T, Osafune T, Kawaguchi A** (1995) Isolation and characterization of mutants affected in lipid metabolism of *Chlamydomonas reinhardtii*. *Eur J Biochem* **230**: 987–993
- Shanklin J, Cahoon EB** (1998) Desaturation and related modifications of fatty acids. *Annu Rev Plant Physiol Plant Mol Biol* **49**: 611–641
- Shimogawara K, Fujiwara S, Grossman A, Usuda H** (1998) High-efficiency transformation of *Chlamydomonas reinhardtii* by electroporation. *Genetics* **148**: 1821–1828
- Siaut M, Cuiné S, Cagnon C, Fessler B, Nguyen M, Carrier P, Beyly A, Beisson F, Triantaphyllidès C, Li-Beisson Y, et al** (2011) Oil accumulation in the model green alga *Chlamydomonas reinhardtii*: characterization, variability between common laboratory strains and relationship with starch reserves. *BMC Biotechnol* **11**: 7
- Silflow CD, LaVoie M, Tam LW, Tousey S, Sanders M, Wu WC, Borodovsky M, Lefebvre PA** (2001) The Vfl1 protein in *Chlamydomonas* localizes in a rotationally asymmetric pattern at the distal ends of the basal bodies. *J Cell Biol* **153**: 63–74
- Sizova I, Fuhrmann M, Hegemann P** (2001) A *Streptomyces rimosus* aphVIII gene coding for a new type phosphotransferase provides stable antibiotic resistance to *Chlamydomonas reinhardtii*. *Gene* **277**: 221–229
- Sperling P, Ternes P, Zank TK, Heinz E** (2003) The evolution of desaturases. *Prostaglandins Leukot Essent Fatty Acids* **68**: 73–95
- Tardif M, Atteia A, Specht M, Cogne G, Rolland N, Brugière S, Hippler M, Ferro M, Bruley C, Peltier G, et al** (2012) PredAlgo: a new subcellular localization prediction tool dedicated to green algae. *Mol Biol Evol* **29**: 3625–3639
- Tasaka Y, Gombos Z, Nishiyama Y, Mohanty P, Ohba T, Ohki K, Murata N** (1996) Targeted mutagenesis of acyl-lipid desaturases in *Synechocystis*: evidence for the important roles of polyunsaturated membrane lipids in growth, respiration and photosynthesis. *EMBO J* **15**: 6416–6425
- Terashima M, Specht M, Hippler M** (2011) The chloroplast proteome: a survey from the *Chlamydomonas reinhardtii* perspective with a focus on distinctive features. *Curr Genet* **57**: 151–168
- Tolletter D, Ghysels B, Alric J, Petroutsos D, Tolstygina I, Krawietz D, Happe T, Auroy P, Adriano JM, Beyly A, et al** (2011) Control of hydrogen photoproduction by the proton gradient generated by cyclic electron flow in *Chlamydomonas reinhardtii*. *Plant Cell* **23**: 2619–2630
- Wallis JG, Browse J** (2002) Mutants of *Arabidopsis* reveal many roles for membrane lipids. *Prog Lipid Res* **41**: 254–278
- Wijffels RH, Barbosa MJ** (2010) An outlook on microalgal biofuels. *Science* **329**: 796–799
- Winter D, Vinegar B, Nahal H, Ammar R, Wilson GV, Provart NJ** (2007) An “Electronic Fluorescent Pictograph” browser for exploring and analyzing large-scale biological data sets. *PLoS ONE* **2**: e718
- Work VH, D’Adamo S, Radakovits R, Jinkerson RE, Posewitz MC** (2012) Improving photosynthesis and metabolic networks for the competitive production of phototroph-derived biofuels. *Curr Opin Biotechnol* **23**: 290–297
- Work VH, Radakovits R, Jinkerson RE, Meuser JE, Elliott LG, Vinyard DJ, Laurens LML, Dismukes GC, Posewitz MC** (2010) Increased lipid accumulation in the *Chlamydomonas reinhardtii* *sta7-10* starchless isoamylase mutant and increased carbohydrate synthesis in complemented strains. *Eukaryot Cell* **9**: 1251–1261
- Yoon K, Han D, Li Y, Sommerfeld M, Hu Q** (2012) Phospholipid:diacylglycerol acyltransferase is a multifunctional enzyme involved in membrane lipid turnover and degradation while synthesizing triacylglycerol in the unicellular green microalga *Chlamydomonas reinhardtii*. *Plant Cell* **24**: 3708–3724
- Zäuner S, Jochum W, Bigorowski T, Benning C** (2012) A cytochrome b5-containing plastid-located fatty acid desaturase from *Chlamydomonas reinhardtii*. *Eukaryot Cell* **11**: 856–863

## **Supplemental MATERIALS AND METHODS**

### **Chlorophyll Quantification**

Total chlorophyll was quantified based on its fluorescence. Chlorophyll was extracted from cell pellet using 100% methanol. After being centrifuged at 10 000 *g* for 5 min at 4°C, the absorbances of the supernatant were read with an UV-visible recording spectrophotometer (Schimadzu UV-260). Chlorophyll content was calculated based on the absorbance at 665 nm for chlorophyll *a* and at 652 nm for chlorophyll *b* according to the formula described in (Lichtenthaler, 1987).

### **Genetic Crosses and Tetrad Dissection**

For identified mutants with desirable lipid phenotypes (*mt*<sup>-</sup>), to clean up its genetic background, the mutant is normally backcrossed with the wild-type CC125 (*mt*<sup>+</sup>). Genetic crosses were performed following the protocol described by Jiang and Stern (Jiang and Stern, 2009). Briefly, *Chlamydomonas* strain of *mt*<sup>-</sup> and *mt*<sup>+</sup> were cultivated in TAP medium up to mid-log phase. Cells were gently centrifuged at 360 *g* for 3 min at room temperature, washed twice with TAP-N medium and resuspended in the same medium. Cultures were kept in TAP-N for 24 h at 25°C under shaking. Cells with opposite mating types were mixed together in a glass tube (1 mL:1 mL) and then the tubes were kept in a incline position in a laminar hood for 3 h. The mixture (1 mL) was then spread into center of TAP plates containing 3% agar (w/v), the plates were dried and kept under low light for overnight. Then the plates were wrapped in aluminum foil, kept in the dark for 5-10 days to induce zygote germination upon induction by light. All the vegetative cells were scraped from the plate with a dull scalpel. To further eliminate the vegetative cells, the plates were exposed to chloroform vapor for 20-45 s. The plates were then placed under low light for 24 h. The tetrads were dissected using a micromanipulator needle connected to a light microscopy under a laminar hood.

### **DNA Extraction from *Chlamydomonas reinhardtii* and Southern Blotting**

Total DNA was prepared from *Chlamydomonas* cells grown at mid-log phase following the protocol of Tolleter (Tolleter et al., 2011). After extraction and purification, DNA was finally suspended into 50 µL of double distilled water. A hybridization probe against cassette *aphVIII* was labeled with Digoxigenin-dUTP (DIG, Roche) by PCR. Before hybridization, the probe was denatured by heating at 100°C for 10 min, and then kept on ice for 5 min. Genomic DNA (~8 µg) was digested overnight by *NotI*, *StuI*, *ApaI* or *XmaI* (NEB). Digested DNA was loaded onto a 0.8% agarose gel, each lane representing DNA cut by one specific enzyme and

the gel was run slowly at 50 V to better separate fragmented DNA. The migration, hybridization and revelation were following the protocol described in (Sambrook and Russell, 2001).

### Phylogenetic Analyses

Homologous amino acid sequences for fatty acid desaturases from cyanobacteria, microalgae, mosses and higher plants were retrieved from Cyanobase (<http://genome.kazusa.or.jp/cyanobase/>), JGI (<http://www.jgi.doe.gov/>), TAIR (<http://www.arabidopsis.org/>), Phytozome (<http://www.phytozome.net/>) or NCBI (<http://www.ncbi.nlm.nih.gov/>). They were aligned using MAFFT v.7 (Kato and Standley, 2013). The resulting alignment was manually refined using SeaView v.4 (Gouy et al., 2010). Phylogenetic analyses were conducted using MEGA5 (Tamura et al., 2011). The Neighbor Joining (NJ) method based on the Jones-Taylor-Thornton (JTT) amino acid substitution model was used. The robustness of tree topology was conducted using bootstrap with 100 replications. The result was confirmed by maximum-likelihood (ML) and parcimony (PARS) analyses. The identities of the selected protein sequences used for the analyses are shown in **Supplemental Table S2**.

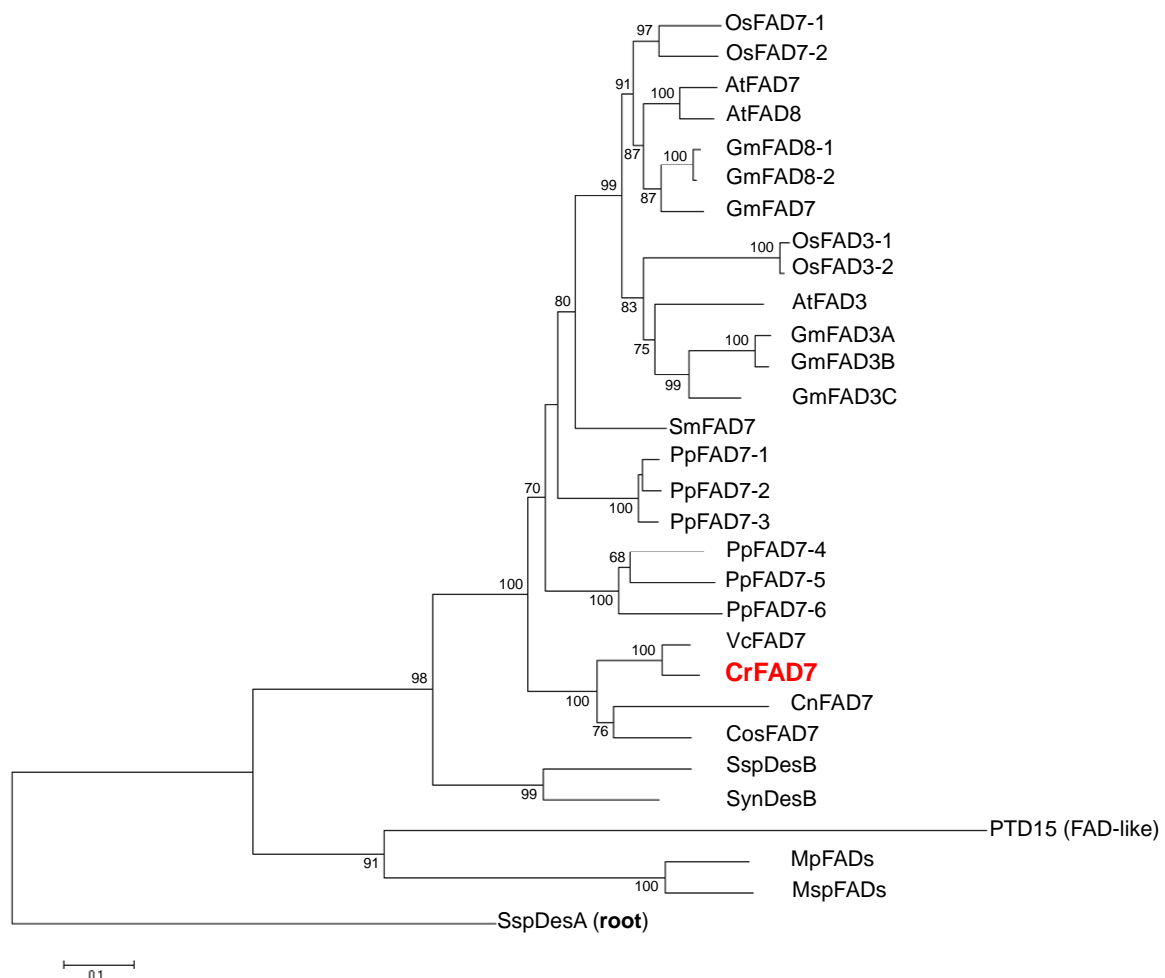
### Supplementary REFERENCES

- Gouy M, Guindon S, Gascuel O** (2010) SeaView Version 4: A Multiplatform Graphical User Interface for Sequence Alignment and Phylogenetic Tree Building. *Molecular Biology and Evolution* **27**: 221-224
- Jiang X, Stern D** (2009) Mating and tetrad separation of *Chlamydomonas reinhardtii* for genetic analysis. *J Vis Exp* **30**: 1274. doi: 10.3791/1274
- Kato K, Standley DM** (2013) MAFFT Multiple Sequence Alignment Software Version 7: Improvements in Performance and Usability. *Molecular Biology and Evolution* **30**: 772-780
- Lichtenthaler H** (1987) Chlorophylls and carotenoids - pigments of photosynthetic biomembranes. *Method Enzymol* **148**: 350 - 382
- Sambrook J, Russell DW** (2001) *Molecular cloning : a laboratory manual*. Cold Spring Harbor, N.Y. : Cold Spring Harbor Laboratory, 2<sup>nd</sup> edition
- Tamura K, Peterson D, Peterson N, Stecher G, Nei M, Kumar S** (2011) MEGA5: Molecular Evolutionary Genetics Analysis Using Maximum Likelihood, Evolutionary Distance, and Maximum Parsimony Methods. *Molecular Biology and Evolution* **28**: 2731-2739
- Tolter D, Ghysels B, Alric J, Petroutsos D, Tolstygina I, Krawietz D, Happe T, Auroy P, Adriano JM, Beyly A, Cuine S, Plet J, Reiter IM, Genty B, Cournac L, Hippler M, Peltier G** (2011) Control of Hydrogen Photoproduction by the Proton Gradient Generated by Cyclic Electron Flow in *Chlamydomonas reinhardtii*. *Plant Cell* **23**: 2619-2630

**Supplementary Table S2. Phylogenetic analysis of fatty acid desaturases (FAD) in oxygenic photosynthetic organisms.**

Sequences were aligned with the MAFFT (v.7) program. List of protein IDs used was listed in the table below after the phylogenetic tree. Neighbor-joining method was used to construct the cladogram. *SspDesA* is used as a root. The *scale bar* represents amino acid changes per position. The trees were obtained with the Neighbour-Joining method. The bootstrap value is shown on each node (obtained from 100 replicates). The confidence of nodes was also supported by analyses with the Maximum Likelihood and Parsimony methods.

Abbreviations: At: *Arabidopsis thaliana*; Cr: *Chlamydomonas reinhardtii*; Cn: *Chlorella* NC64A; Cv: *Chlorella vulgaris* (*Coccomyxa subellipsoidea* C-169); Gm: *Glycine max*; Pp: *Physcomitrella patens*; Sm: *Selaginella moellendorffii*; Ssp: *Synechocystis sp.* PCC 6803; Syn: *Synechococcus sp.* PCC 7002; Vc: *Volvox carteri*; Os: *Oryza sativa japonica*; Mp: *Micromonas pusilla* CCMP1545 v1.0; Msp: *Micromonas sp.* RCC299 v3.0; Pt: *Phaeodactylum tricornutum* CCAP 1055/1.

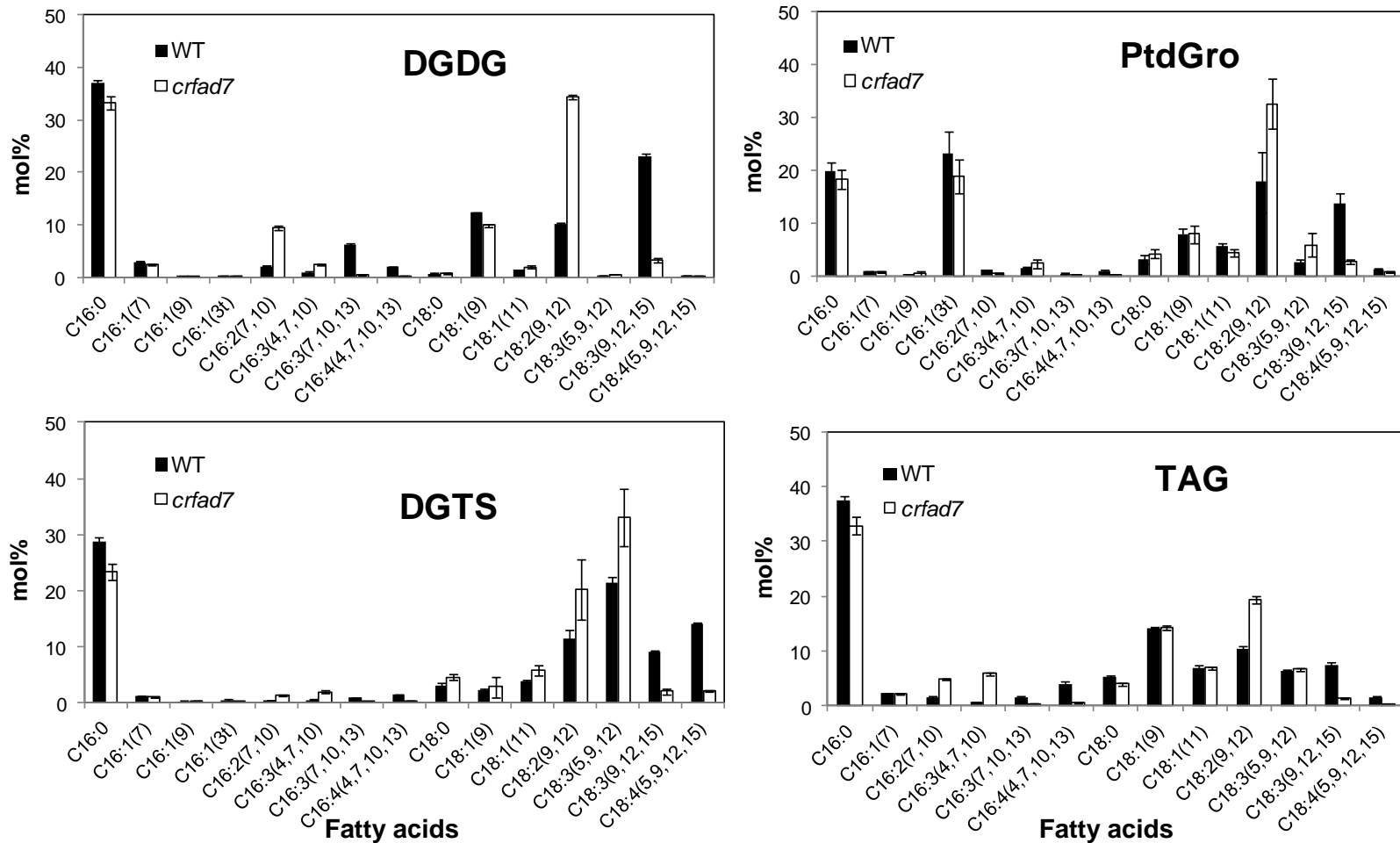


List of IDs for protein sequences and their abbreviations used to construct the phylogenetic tree presented above.

	Abbreviation	Organism	ID
Plant eudicots	AtFAD3	<i>Arabidopsis thaliana</i>	AT2G29980
	AtFAD7	<i>Arabidopsis thaliana</i>	AT3G11170
	AtFAD8	<i>Arabidopsis thaliana</i>	AT5G05580
	GmFAD3B	<i>Glycine max</i>	Glyma02g39230
	GmFAD3C	<i>Glycine max</i>	Glyma18g06950
	GmFAD8	<i>Glycine max</i>	Glyma03g07570
	GmFAD8-1	<i>Glycine max</i>	Glyma01g29630
	GmFAD7	<i>Glycine max</i>	Glyma07g18350
	GmFAD3A	<i>Glycine max</i>	Glyma14g37350
Plant monocots	OsFAD7-1	<i>Oryza sativa Japonica Group</i>	ABF95395
	OsFAD7-2	<i>Oryza sativa Japonica Group</i>	NP_001060733
	OsFAD3-2	<i>Oryza sativa Japonica Group</i>	NP_001065926
	OsFAD3-1	<i>Oryza sativa Japonica Group</i>	ABA91057
Bryophyta	SmFAD7	<i>Selaginella moellendorffii</i>	103593
	PpFAD7-1	<i>Physcomitrella patens</i>	Phpat.017G055900
	PpFAD7-2	<i>Physcomitrella patens</i>	Phpat.017G066400
	PpFAD7-3	<i>Physcomitrella patens</i>	Phpat.014G100000
	PpFAD7-4	<i>Physcomitrella patens</i>	Phpat.013G032600
	PpFAD7-5	<i>Physcomitrella patens</i>	Phpat.003G032600
	PpFAD7-6	<i>Physcomitrella patens</i>	Phpat.026G038000
Green microalgae	CrFAD7	<i>Chlamydomonas reinhardtii</i>	Cre01.g038600
	VcFAD7	<i>Volvox carteri</i>	Vocar20009411m.g
	CosFAD7	<i>Coccomyxa subellipsoidea C-169 (Chlorella vulgaris)</i>	estExt_Genemark1.C_130077
	CnFAD7	<i>Chlorella NC64A</i>	estExt_Genewise1.C_430002
	MpFADs	<i>Micromonas pusilla CCMP1545 v1.0</i>	e_gw1.15.141.1
	MspFADs	<i>Micromonas sp. RCC299 v3.0</i>	fgenes2_pg.C_Chr_13000212
	Diatom	PTD15 (FAD-like)	<i>Phaeodactylum tricorutum</i> CCAP 1055/1
Cyanobacteria	SspDesB	<i>Synechocystis sp. PCC 6803</i>	s111441
	SspDesA	<i>Synechocystis sp. PCC 6803</i>	NP_441489
	SynDesB	<i>Synechococcus sp. PCC 7002</i>	SYNPCC7002_A0159

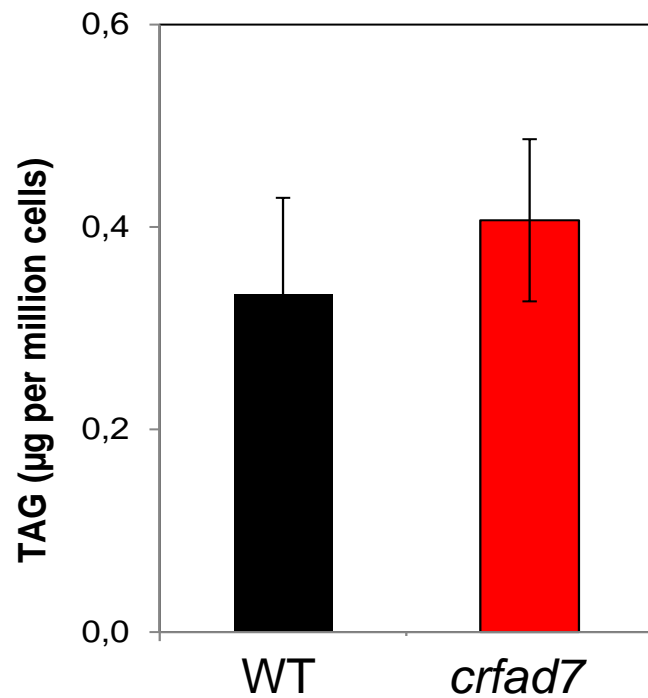
**Supplementary Table S3.** All primers and their sequences used in this study.

Purpose	Name	Primer sequences (5'-3')
For qRT-PCR	<i>fad7 F</i>	CGGCCACCAGTCTTTCTCAA
	<i>fad7 R</i>	TGGTCGTACAGCTTCTTGGTCA
	<i>rack1 F</i>	CTTCTCGCCCATGACCAC
	<i>rack1 R</i>	CCCACCAGGTTGTTCTTCAG
Gene expression, protein localization and complementation related	<i>NdeI-Fad7-F1</i>	ACATATGAGATGCAGTGCCTGTCTCG
	<i>EcoRV-Fad7-R1</i>	AGATATCGCCGTGCCAGAGTCTAAC
	<i>inF HA Fw</i>	ATCCACTAGTTCTAGCCTGTCGCGATACCCCTAC
	<i>inF HA Rev</i>	CTGCTGCCATCTAGCTAACTGCTAGCGGCGTAGTC
	<i>InF FAD7 Fw</i>	TCGATAAGCTTGATATGCAGTGCCTGTCTCGCTCC
	<i>InF FAD7 Rev</i>	CTGCAGGAATTCGATGGCCTTGCCGGCAACCGCCTTGC

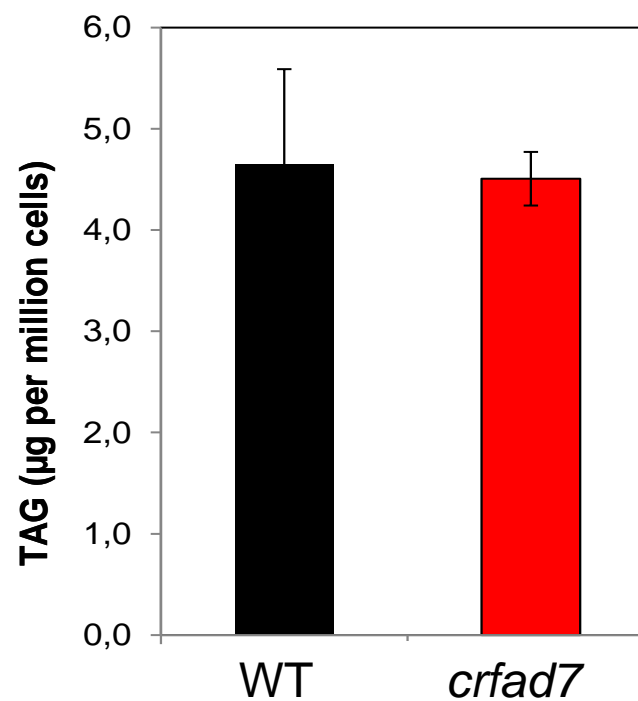


**Supplemental Figure S1.** Fatty acid compositions (mol%) for individual lipid classes after being separated by Thin Layer Chromatography (TLC) were shown. Data are means of three replicates  $\pm$  standard deviation (n=3). Shown are DGDG, digalactosyldiacylglycerol; DGTS, 1,2-diacylglyceryl-3-O-4'-(N,N,N-trimethyl)-homoserine; PtdGro, phosphatidylglycerol and TAG, triacylglycerol.

### A. TAP



### B. TAP-N

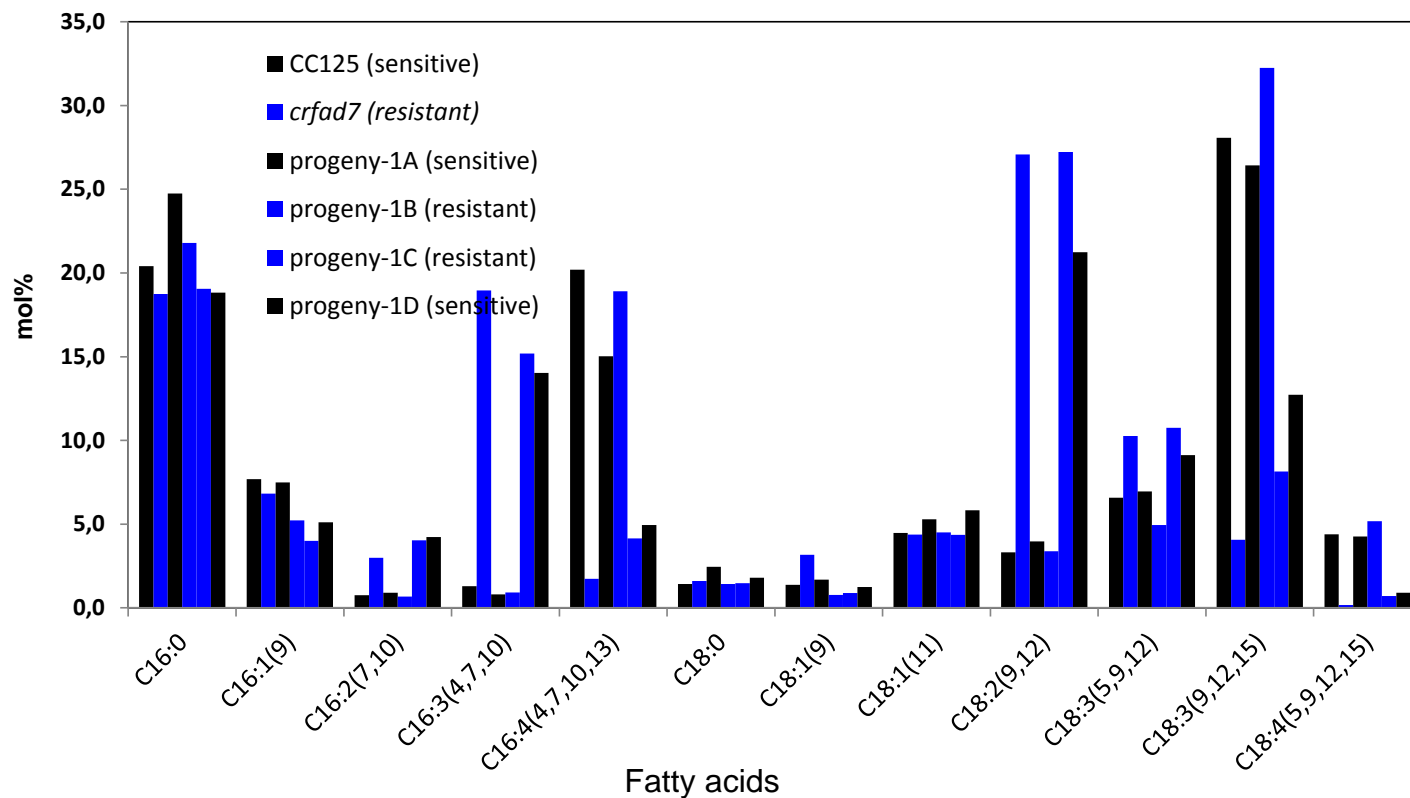


**Supplemental Figure S2.** Comparison of triacylglycerol (TAG) content between WT and the mutant *crfad7* under (A) standard growth conditions and (B) nitrogen starvation for 48 h. Cells were grown to exponential phase, and then changed to nitrogen free media for another 48 h before cells were harvested for lipid extraction and TAG quantification. Data are mean  $\pm$  standard deviation (n=3).

**A** WT *crfad7*



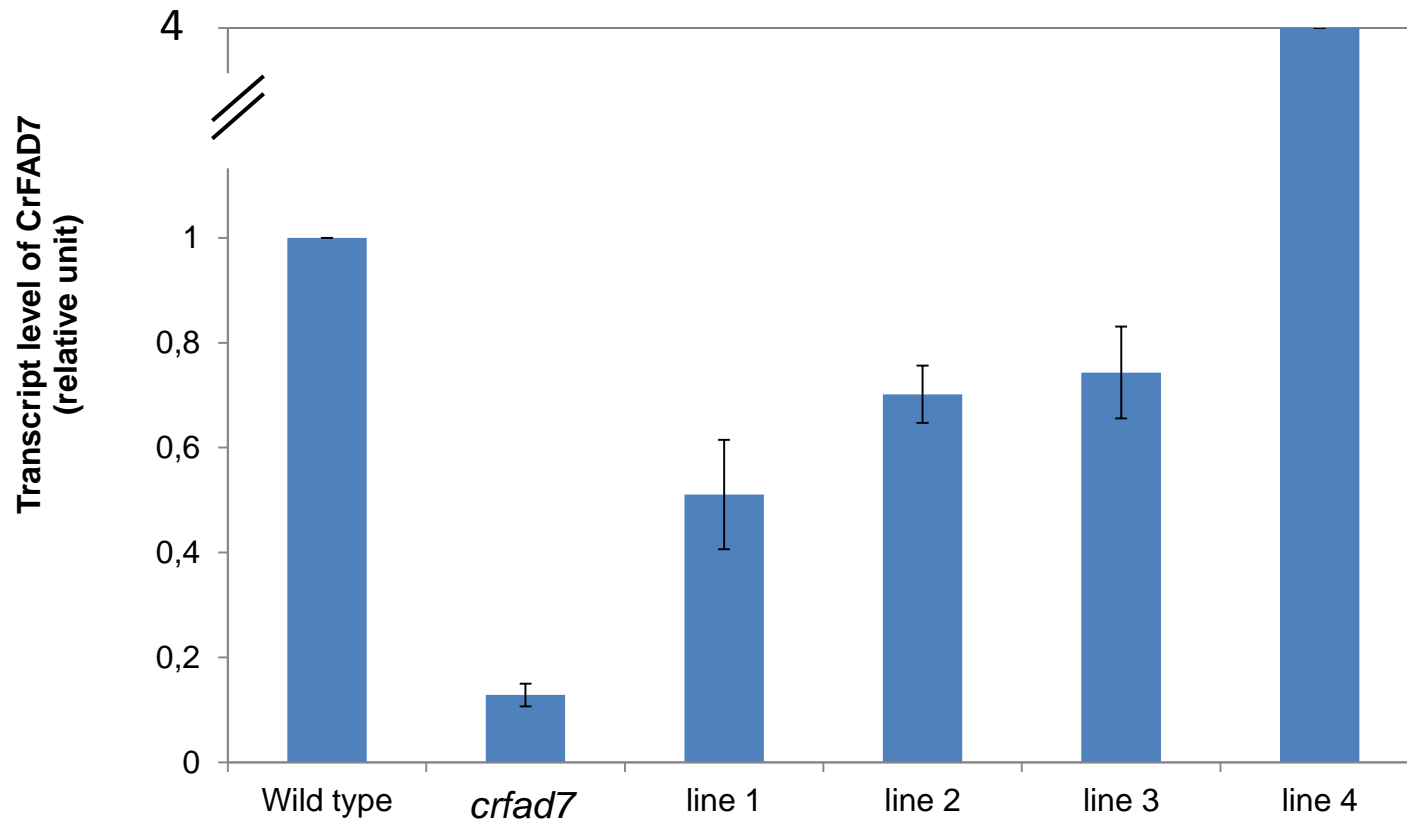
**B**



**Supplemental Figure S3.** Analysis of the number of *aphVIII* insertions and linkage between altered fatty acid phenotype and paromomycin resistance.

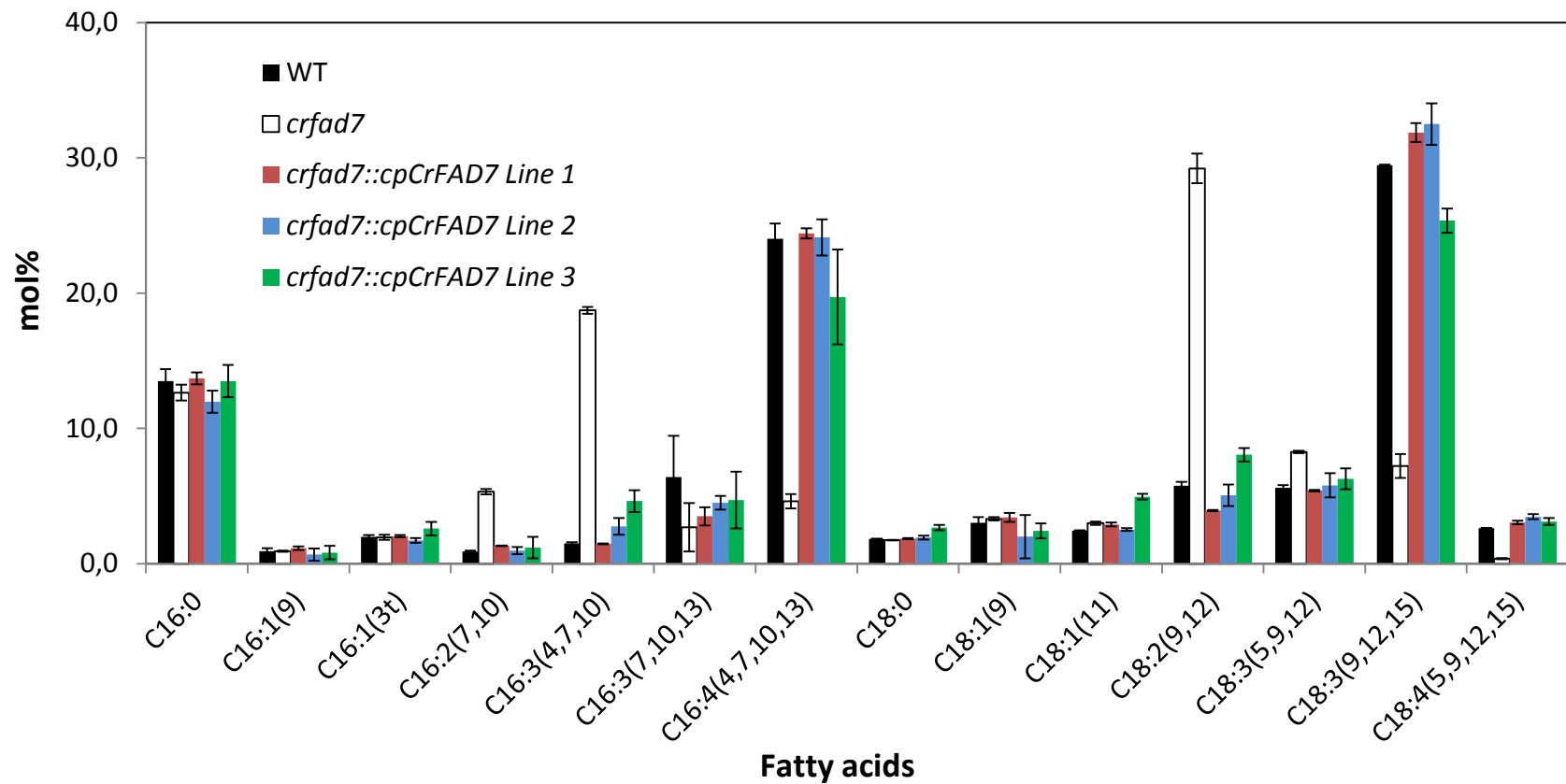
(A). Southern blot analysis of the *crfad7* genome revealed at least 2 *aphVIII* insertions. Genomic DNA of WT and *crfad7* mutant were digested by *NotI*, and then blotted against a probe containing the gene *aphVIII*.

(B). Fatty acid composition of the progeny of one complete tetrad obtained from the genetic crosses between 1C11 (*mt*) and CC125 (*mt+*). Note: Paromomycin resistant clones are shown in blue; non-resistant clones are shown in black.



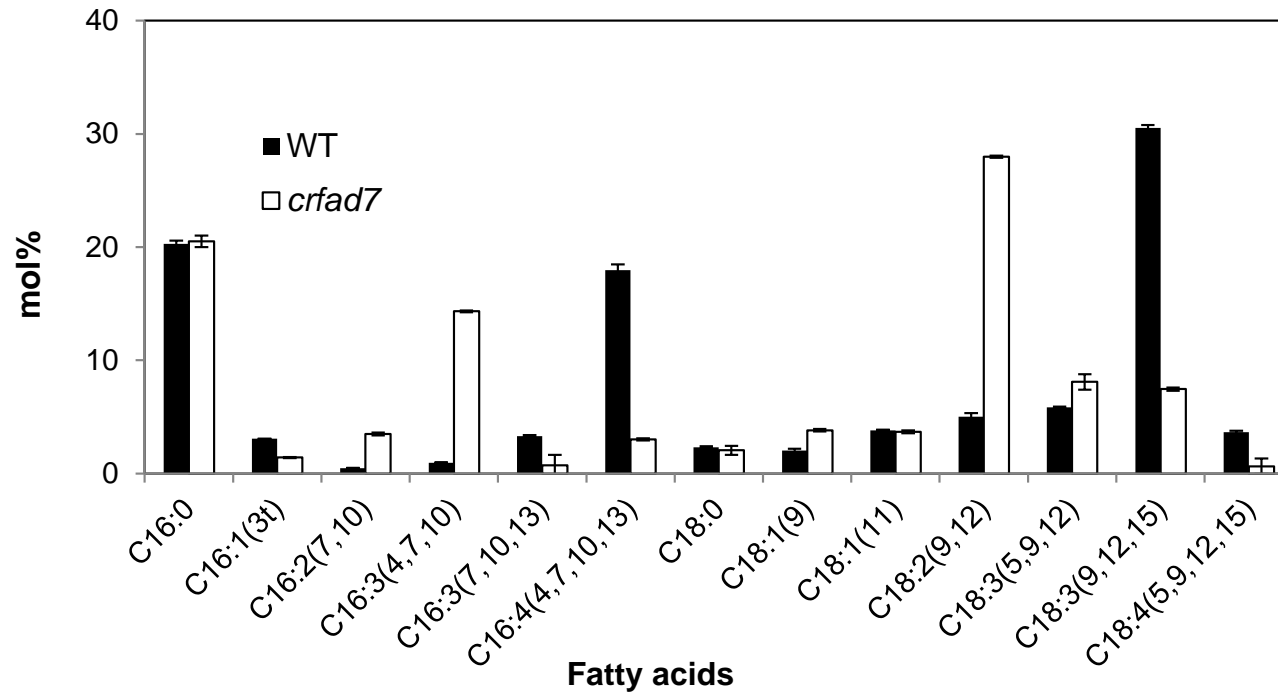
**Supplemental Figure S4.** Quantitative RT-PCR analyses of the transcription level of *CrFAD7* in WT, the mutant *crfad7*, and four nuclear complemented lines.

Expression levels of Cre01.g038600 (*CrFAD7*) were first normalized to the housekeeping gene *RACK1*. The expression level is compared to that of WT (set at 1). Error bars represent standard deviation based on three biological replicates, each biological replicate consisting of three technical replicates.

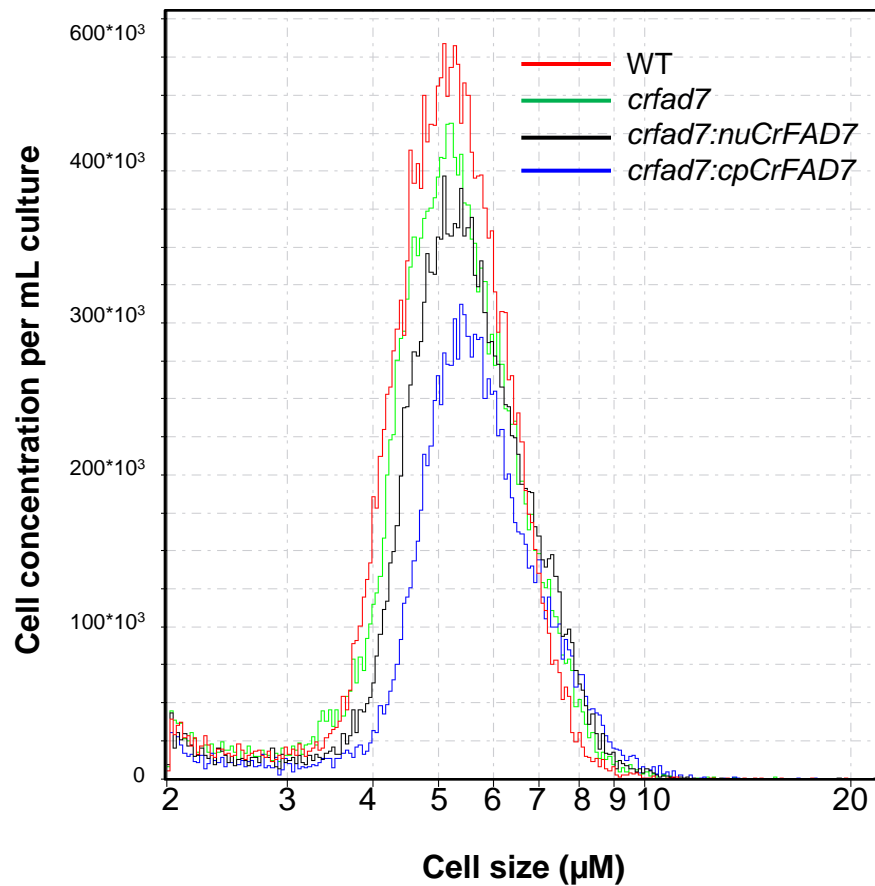
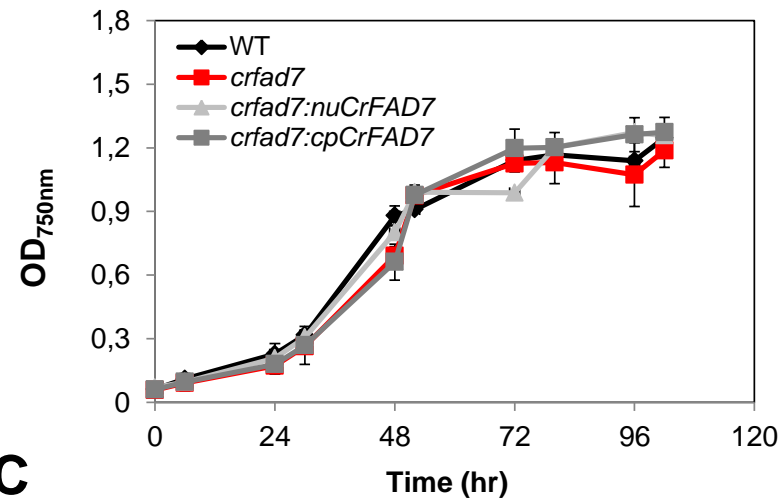
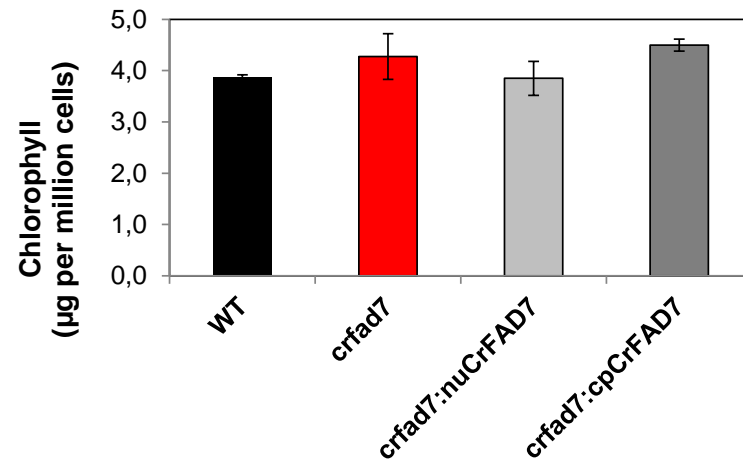


**Supplemental Figure S5.** Fatty acid methyl ester (FAME) analyses of several complemented lines of the mutant *crfad7* by plastidial transformation of a codon-adapted *CrFAD7* gene. Data represent average of three biological replicates, and error bars represent 95% confidence intervals (CIs). Three independent transformants were compared to WT and *crfad7*.

At 15°C



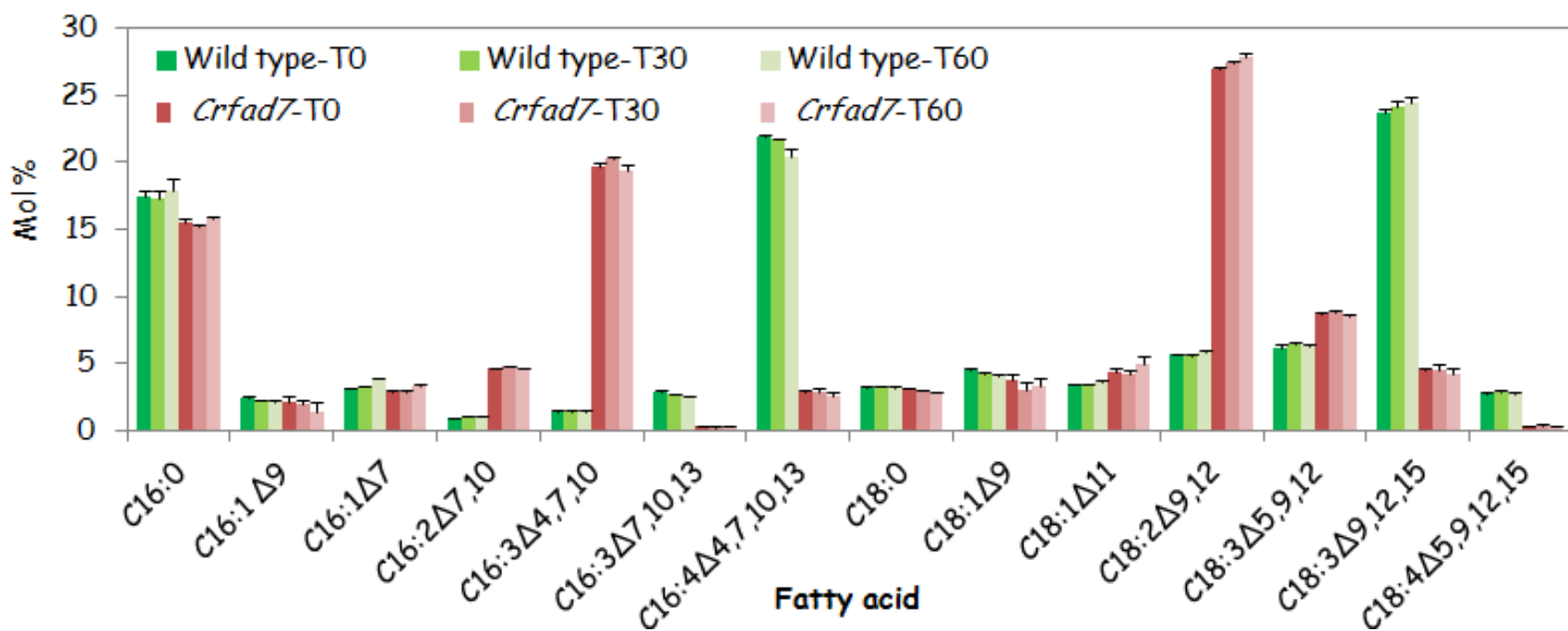
**Supplemental Figure S6.** Proportions (mol%) of fatty acids in the WT and mutant *cfad7* when cultivated at a temperature of 15°C. Data are means of three biological replicates, with error bars representing standard deviations (n=3).

**A****B****C**

**Supplemental Figure S7.** Comparison of cell size, growth kinetics and chlorophyll content between WT, *crfad7*, and the two complemented lines (*crfad7:nuCrFAD7*, *crfad7:cpCrFAD7*). *nu*: nuclear; *cp*: chloroplast.

Cells of WT and *crfad7* were grown in regular TAP medium until mid-log phase, and were inoculated into fresh medium to reach an optical density at 750 nm (OD<sub>750nm</sub>) of 0.05. Then 1 mL culture were taken at regular time point for counting. In parallel, cells were also counted with a cell counter, which gave cell size measurement as well as growth curve (data not shown). A similar kinetics of cell growth was also observed between WT and the mutant *crfad7* (data not shown).

Data are means ± standard deviation. Three biological replicates were analyzed for each time point.



**Supplemental Figure S8.** Fatty acid compositions remains constant during short-term heat stress (45°C) for both WT and *crfad7*, but the difference between WT and the mutant *crfad7* remain constant at elevated temperatures. Data are means of three biological replicates, and error bars represent standard deviations (n=3). T0: representing starting point, T30: 30 min after heat stress; T60, 60 min after heat stress.